v3 Integrin is Required for Efficient Infection of Epithelial Cells with Human 1 Adenovirus Type 26

TITLE: αvβ3 Integrin is Required for Efficient Infection of Epithelial Cells with Human Adenovirus Type 26

Davor Nestić[1], Taco G. Uil[2], Jiangtao Ma[3], Soumitra Roy[2], Jort Vellinga[2], Andrew H. Baker[4], Jerome Custers[2,#], Dragomira Majhen[1,2,#]

[1]Laboratory for Cell Biology and Signalling, Division of Molecular Biology, Ruđer Bošković Institute, Zagreb, Croatia, [2]Viral Vaccine Discovery and Early Development, Janssen Vaccines and Prevention BV, Leiden, The Netherlands, [3]Glasgow Cardiovascular Research Centre College of Medical, Veterinary and Life Sciences, University of Glasgow, Glasgow, United Kingdom, [4]Centre for Cardiovascular Science, University of Edinburgh, Queen's Medical Research Institute, 47 Little France Crescent, Edinburgh EH16 4TJ, United Kingdom

RUNNING TITLE: αvβ3 Integrin is receptor for Human Adenovirus Type 26

#corresponding authors: Jerome Custers: JCuster1@its.jnj.com, Dragomira Majhen: dmajhen@irb.hr

KEYWORDS: human adenovirus type 26, αvβ3 integrin, receptor, epithelial cells

ABSTRACT

Human adenoviruses (HAdVs) are being explored as vectors for gene transfer and vaccination. Human adenovirus type 26 (HAdV26), which belongs to the largest subgroup of adenoviruses, species D, has a short fiber and a so far unknown natural tropism. Due to its low seroprevalence, HAdV26 has been considered a promising vector for the development of vaccines. Despite the fact that the *in vivo* safety and immunogenicity of HAdV26 has been extensively studied, the basic biology of this virus,

with regard to receptor use, cell attachment, internalization and intracellular trafficking is poorly understood. In this work we investigated the role of the coxsackie- and adenovirus receptor (CAR), CD46 and αv integrins in HAdV26 infection of human epithelial cell lines. By performing different gain- and loss-of-function studies we found that αvβ3 integrin is required for efficient infection of epithelial cells by HAdV26, while CAR and CD46 did not increase transduction efficiency of HAdV26. By studying intracellular trafficking of fluorescently labeled HAdV26 in A549 cells and A549-derived cell clones with stably increased expression of αvβ3 integrin, we observed that HAdV26 co-localizes with αvβ3 integrin and that increased αvβ3 integrin enhances internalization of HAdV26. Thus we conclude that HAdV26 uses αvβ3 integrin as a receptor for infecting epithelial cells. These results give us new insight into the HAdV26 infection pathway and will be helpful in further defining HAdV-based vector manufacturing and vaccination strategies.

IMPORTANCE

Adenovirus-based vectors are used today for gene transfer and vaccination. HAdV26 has emerged as a promising candidate vector for development of vaccines due to its relatively low seroprevalence and its ability to induce potent immune responses against encoded transgenes. However, data regarding the basic biology of this virus, like receptor usage or intracellular trafficking, are limited. In this work we found that efficient infection of human epithelial cell lines by HAdV26 requires the expression of the αvβ3 integrin. By studying intracellular trafficking of fluorescently labeled HAdV26 in a cell clone with stably increased expression of αvβ3 integrin, we observed that HAdV26 co-localizes with αvβ3 integrin and confirmed that αvβ3 integrin expression facilitates

efficient HAdV26 internalization. These results will allow us further improvement of HAdV26 based vectors for gene transfer and vaccination.

INTRODUCTION

Adenoviruses are non-enveloped double-stranded DNA viruses with an icosahedral capsid of approximately 90 nm in diameter and a mass of 150 megadaltons (1). The major building blocks of the adenoviral capsid are the hexon and penton proteins. On each vertex there is an extended fiber protein non-covalently attached to the penton base protein (2). A broad knowledge of adenovirus molecular biology, and the relative ease with which the genome can be manipulated, have made them attractive as vectors for gene transfer and vaccination (3). Adenovirus-based vectors rapidly infect a broad range of human cells and induce strong innate responses (4) that positively influence adaptive T- and B- cell responses (5). Adenovirus-based vectors currently represent a leading choice for vectors used in gene therapy clinical trials aimed at treating inherited diseases, infections and cancer (http://www.abedia.com/wiley/vectors.php).

Human adenoviruses belong to *Mastadenovirus* genus of the *Adenoviridae* family and comprise more than 60 distinct serotypes divided into 7 species or subgroups (A-G) (6-8). The most common and best described HAdV so far is the species C human adenovirus type 5 (HAdV5). HAdV5 infection starts with binding to coxsackie adenovirus receptor (CAR) followed by interaction between the RGD sequence motif present on the penton base with the αv integrins on the cell surface, allowing internalization of the viral particle (9). HAdV5 is very efficient with respect to *in vitro* transduction efficiency and level of gene expression; however its disadvantage is the high level and frequency of preexisting immunity in human populations. The seroprevalence of HAdV5 ranges from

50–90% depending on the geographical region (10, 11). Preexisting immunity may limit the efficiency of adenovirus-based vaccine vectors, and thus development of new strategies to evade undesired anti-vector host immune responses, such as vectors based on adenoviruses that occur at low prevalence in human populations, is needed. Some of the rare human adenovirus types that are under evaluation include HAdV35 (species B) and HAdV26 (species D) as well as adenoviruses from non-human primates (12, 13). Vaccine vectors based on HAdV26 and HAdV35 have been extensively studied and are listed as interventions in more than 40 clinical trials, either alone or in prime-boost regime (https://clinicaltrials.gov).

As mentioned above, HAdV26 belongs to species D, the largest group of HAdVs (14), that are mainly known to be responsible for eye infections and for gastro-intestinal infections in immuno-compromised individuals. Similarly to the majority of HAdVs, HAdV26 has RGD motifs in the penton base that can mediate integrin binding. In contrast to HAdV5 which has a long fiber containing 22 beta-repeat motifs, HAdV26 has a relatively short fiber with only 8 beta repeats (15). Also, unlike HAdV5, HAdV26 does not bind coagulation factor X (16).

Although the safety and immunogenicity of HAdV26-based vaccine vectors *in vivo* is well established (17-20), the basic biology of this virus, such as receptor usage, is less well understood. Several molecules have been identified as cellular receptors for HAdVs (21). As discussed above, HAdV5 from species C uses CAR as primary receptor for facilitating entry into cells (22) while HAdV35 from species B utilizes CD46 as the primary receptor (23). HAdV5 uses also αv integrins as co-receptors mediated by an interaction with the RGD sequence in the penton base (24). Integrins are heterodimers

of non-covalently associated α and β subunits assembled into 24 different receptors. They are major receptors for cell adhesion to extracellular matrix proteins and activate many intracellular signaling pathways after binding to cognate ligands. With respect to HAdV26, several studies have reported that HAdV26 utilizes CAR, CD46 and/or integrins as receptors for infecting target cells *in vitro*. Abbink *et al.* reported that HAdV26 transduces B16F10-CD46 cells, mouse B16F10 melanoma cells that stably express the BC1 isoform of human CD46 on the membrane, more efficiently than B16F10 cells indicating that HAdV26 is able to utilize CD46 as a receptor. However, transduction appeared less efficient than for HAdVs from species B, suggesting that HAdV26 may utilize other receptors in addition to CD46 (20). Recently, it has been shown that HAdV26 uses CD46 as a primary receptor in human peripheral blood mononuclear cells, and that HAdV26 transduction was efficiently blocked by an anti-CD46 monoclonal antibody (25).

Chen *et al*. compared the transduction efficiencies of HAdV5 and HAdV26 in CHO cells (cell line originally derived from the Chinese hamster ovary) stably expressing CAR (CHO-CAR) and control cells which do not express CAR (CHO-HVEM). They observed that at the higher dose tested, transduction efficiencies of the two viruses were similar in CHO-CAR cells indicating that HAdV26 could utilize CAR for cell binding. At the same time transduction in CHO-HVEM cell line by HAdV26 was higher than by HAdV5, suggesting that HAdV26 can enter cells upon binding to alternative receptors that HAdV5 is unable to use. In the same study, the authors investigated the agglutination of CD46-expressing red blood cells from rhesus macaques by HAdV26. A species B chimpanzee adenovirus serotype C1 – based vector, which had previously been shown

to bind CD46, readily agglutinated red blood cells from rhesus macaques, whereas this was not seen with HAdV26, suggesting that HAdV26 did not bind CD46 (26). Another study found that cyclic-RGD peptides partially inhibited human hepatoma Hep3B cell killing by HAdV26 indicating a role of αv integrins in HAdV26 infection. In the same study, the combination of an anti-CD46 antibody and cyclic-RGD peptides on patient myeloma cells mediated complete protection against killing by HAdV26, suggesting that both receptors, CD46 and αv integrins, are being utilized by the virus to infect these target cells (27). Finally, very recently the scavenger receptor SR-A6 has been implicated in facilitating HAdV26 entry into murine alveolar macrophage-like MPI cells (28). HAdV26 receptor usage has also been investigated for peripheral blood mononuclear cells (25) or malignant B cells (27), while HAdV26 receptor usage in epithelial cells is less well defined.

Since HAdV26 has been reported to use different molecules for cell entry, we wished to investigate the roles of CAR, CD46 and αv integrins in mediating the entry of HAdV26 into human epithelial cells. By performing different gain- and loss-of-function studies we found that αvβ3 integrin is necessary for the efficient infection of epithelial cells by HAdV26. At the same time presence of CAR or CD46 did not increase transduction efficiency of HAdV26. By studying intracellular trafficking of fluorescently labeled HAdV26 in A549 cells and in A549 cells with increased expression of αvβ3 integrin, we observed that αvβ3 integrin expression allows better internalization of HAdV26. Additionally, we have shown that in an A549 cell clone with increased αvβ3 integrin expression HAdV26 co-localizes with αvβ3 integrin. Thus we conclude that HAdV26 uses αvβ3 integrin as a receptor for infecting epithelial cells.

RESULTS

HAdV26 binds and infects A549 and SK-OV-3 cells less efficiently than HAdV5 and HAdV35. Studies regarding HAdV26 transduction efficiency and receptor usage in epithelial cells are limited. Therefor in this work we investigated transduction efficiency of HAdV26 in A549 and SK-OV-3 epithelial cell lines which are often used in adenovirus research. Several molecules have been reported to function as HAdV26 receptors so far: CAR, CD46 and αv integrins. In order to determine the expression level of these molecules on A549 and SK-OV-3 cells we assessed the expression of CAR, CD46, and the integrins αv, αvβ3 and αvβ5 on the surface of these cells by flow cytometry. While SK-OV-3 cells were found to be CAR negative, A549 cells showed high expression of CAR. A549 and SK-OV-3 cells both showed high expression of CD46 and αv integrins; however SK-OV-3 cells express more CD46 and αv integrin than A549. Expression of αvβ3 and αvβ5 integrins, known receptors for the RGD motif which is present in adenovirus penton base, is disparate between these two cell lines. A549 cells express very low amounts of αvβ3 integrin and show expression of αvβ5 integrin, while SK-OV-3 cells express αvβ3 integrin but the level of αvβ5 integrin was very low (Fig. 1).

Next, the efficiency of HAdV26 in transducing A549 and SK-OV-3 was investigated (Fig. 2). HAdV5 and HAdV35 were used as representatives of HAdVs known to utilize the receptors CAR and CD46 respectively. As an additional control, we used HAdV26F35, a chimeric vector based on HAdV26 that has been pseudotyped with the HAdV35 fiber.

HAdV5, HAdV35 and HAdV26F35 were found to transduce A549 cells much better than HAdV26. HAdV26 transduced A549 cells 1000-fold less efficiently than HAdV5. The transduction efficiency of HAdV26 was comparable to HAdV5 in SK-OV-3 cells, i.e.,

HAdV26 transduced SK-OV-3 cells only 3-fold less efficiently than HAdV5 (Fig. 2A). HAdV26 showed 4-fold higher reporter gene expression in SK-OV-3 cells than in A549 cells (Fig.2B). This may indicate that SK-OV-3 cells express higher levels of the molecule/s that HAdV26 uses as a receptor than A549 cells do.

To investigate whether the relatively low level of transduction efficiency observed for HAdV26 in A549 and SK-OV-3 cells (compared to the other vectors) is caused by low binding and/or inefficient internalization of this virus, we measured the binding and internalization of HAdV5, HAdV26, HAdV35 and HAdV26F35 in A549 and SK-OV-3 cells. While the level of binding and internalization of HAdV5, HAdV35 and HAdV26F35 in A549 cells was comparable, binding and internalization of HAdV26 was found to be poor on this cell line. Compared to HAdV5, HAdV26 was found to bind 6-fold and internalize 14-fold less efficiently in A549 cells (Fig. 3A). In SK-OV-3 cells the amount of both bound and internalized HAdV26 was comparable to HAdV5. However, in comparison to AdV35, HAdV26 was less efficient in both binding and internalization in this cell line. In the same cell line HAdV35 and HAdV26F35 were found to bind and internalize more than 10-fold more efficiently than HAdV5 (Fig. 3B). A comparison of the binding and internalization of HAdV26 in A549 and SK-OV-3 cells is shown in Fig. 3C. It was seen that HAdV26 bound 3-fold, and internalized 1.5-fold better to SK-OV-3 cells than to A549 cells. These data indicate that the low transduction efficiency of HAdV26 in A549 cells is caused by decreased binding of this virus, suggesting that this is due to comparatively lower amounts of the HAdV26 receptor on A549 cells.

Downregulation of αv integrin decreases transduction efficiency of HAdV26. To investigate the importance of CAR, CD46 and αv integrin in contributing to the

transduction efficiency of HAdV26 in A549 and SK-OV-3 cells we decided to downregulate those molecules, alone or in combination, and measure the transduction efficiency of HAdV26. To downregulate target receptor/s we transfected cells with CAR-, CD46- and/or αv integrin-specific siRNA (50 nM) and 48 hours post-transfection confirmed the efficiency of silencing by flow cytometry. Downregulation of CAR, CD46 and/or αv integrin was specific and did not influence expression of the other observed molecules (Fig. 4). As expected, downregulating CAR (alone, or in combination with CD46 or αv integrin) almost abolished HAdV5 transduction of A549 cells (Fig. 5A). Silencing of CD46 significantly decreased transduction of HAdV35 (Fig. 5C) and HAdV26F35 (Fig. 5D), but increased transduction of HAdV26 (Fig. 5B). Downregulation of CAR and, to a greater extent, αv integrin decreased the transduction efficiency of both HAdV26 (Fig. 5B) and HAdV26F35 (Fig. 5D). The most prominent effect on HAdV26 transduction was observed in case of αv integrin downregulation which decreased HAdV26 transduction efficiency 3 fold in comparison to cells transfected with the scrambled siRNA control (Fig. 5B). These data indicate that αv integrin could be receptor for HAdV26 in A549 cells. The same effect was observed in another CAR positive cell line, HeLa, where downregulation of αv integrin decreased HAdV26 transduction efficiency 3-fold in comparison to cells transfected with scrambled siRNA (data not shown). Similar results were obtained in SK-OV-3 cells. Since SK-OV-3 cells are CAR negative we downregulated only CD46 and/or αv integrins. Downregulating αv integrin in SK-OV-3 cells decreased transduction efficiency of all 4 studied viruses (Fig. 6); however the decrease was the highest for HAdV26. Downregulating αv integrin in SK-OV-3 cells decreased HAdV26 transduction efficiency 5-fold compared to controls (Fig. 6B). That αv integrin is necessary for HAdV26 transduction efficiency was also

confirmed in melanoma M21 cell line variants M21L and M21L4. The transduction efficiency of HAdV26 was much higher in M21L4 cells which are αv integrin positive, than in M21L cells which are αv integrin negative (Fig. 7).

Downregulating CD46 alone or in combination with αv integrin in SK-OV-3 cells decreased the transduction efficiency of HAdV35 (Fig. 6C) and HAdV26F35 (Fig. 6D), but also HAdV26 (Fig. 6B) indicating that in this cell line CD46 can be involved in HAdV26 transduction efficiency. The role of CAR and CD46 in HAdV26 transduction efficiency was additionally studied in CHO cells overexpressing CAR (CHO-CAR) or CD46 (CHO-BC1). As expected, increased expression of CAR significantly increased transduction efficiency of HAdV5. However there was no impact on the transduction of HAdV26, HAdV35 or HAdV26F35 vectors. Increased expression of CD46 significantly increased the transduction efficiency of HAdV35 and HAdV26F35, but did not change the transduction efficiency of HAdV5 or of HAdV26 (Fig. 8). Based on these data we hypothesize that HAdV26 uses αv integrin as a receptor for infecting epithelial cells, while CAR and CD46 are not crucial molecules in this process.

Downregulation of αv integrin decreases binding and internalization of HAdV26 in A549 cells. To further investigate the roles of CAR, CD46 and αv integrins in HAdV26 infection of A549 cells, we downregulated these molecules and subsequently determined the effect on the binding and internalization of HAdV26 compared to HAdV35 and HAdV26F35. Downregulation of CAR decreased both binding and internalization of HAdV5 4- and 11- fold respectively in comparison to cells transfected with scrambled siRNA (control). Downregulation of CD46 decreased the binding of HAdV35 3-fold and HAdV26F35 5-fold compared to controls. As expected,

downregulation of CD46 also diminished internalization of HAdV35, but surprisingly had no effect on HAdV26F35 internalization. Downregulation of αv integrin significantly decreased binding and internalization of HAdV26. While downregulating αv integrin decreased HAdV26 binding 3-fold, it almost completely abrogated internalization of this virus in A549 cells. Downregulating CAR or CD46 had no influence on HAdV26 binding or internalization (Fig. 9). These data confirm that αv integrin plays an important role in binding and internalization of HAdV26 in A549 cells.

Blocking αv integrins decreases transduction efficiency of HAdV26 in A549 cells. While downregulating target receptors by the use of the specific siRNA removes the target mRNA, and hence the protein from the cell, pharmacological inhibition by using a specific inhibitor or antibody blocks the function of a protein without affecting protein expression. Thus we decided to investigate the role of cell surface CAR, CD46 and/or αv integrins in HAdV26 transduction efficiency by reducing the accessibility of these molecules by blocking antibodies. Blocking CD46 alone or in combination with blocking CAR and αv integrins efficiently decreased transduction of HAdV35 and HAdV26F35 (Fig. 10C, Fig. 10D). This effect was very pronounced for HAdV26F35 where blocking CD46 almost abrogated HAdV26F35 transduction efficiency in A549 cells. Blocking CD46 had no influence on HAdV26 transduction efficiency. The transduction efficiency of HAdV5 was influenced only by blocking CAR, alone or in combination with blocking αv integrins (Fig. 10A). Blocking the surface availability of αv integrins, alone or in combination with both CAR and CD46, significantly decreased the transduction efficiency of HAdV26. While blocking αv integrins alone or in combination with CAR decreased HAdV26 transduction efficiency 2-fold (compared to cells incubated with an

irrelevant IgG), blocking αv integrins and CD46 at the same time decreased HAdV26 transduction efficiency 5-fold (Fig. 10B). Together these results confirm that presence of αv integrin on the surface of A549 is important for transduction efficiency of HAdV26.

Overexpression of αvβ3 integrin in A549 cells allows better transduction efficiency and internalization of HAdV26. To further confirm the role of αv integrins in transduction efficiency of HAdV26 we decided to stably transfect A549 cells with an αv integrin expression plasmid. We isolated three A549 cell clones with increased expression of αv integrin on the cell surface: A549-D4, A549-F1 and A549-E6. Among them, A549-E6 has the highest expression of αv integrins (Fig. 11A). In order to determine if this increased expression of αv integrins has an influence on HAdV26 binding we incubated A549, A549-D4, A549-F1 and A549-E6 cells with HAdV26 and measured the binding of this virus by qPCR. In comparison to A549, HAdV26 binds slightly better to all three clones, namely 1.7-fold better to A549-D4 and A549-E6, and 1.3-fold better to the A549-F1 clone (Fig. 12A). However increased internalization was observed only in clone A549-E6 in which HAdV26 internalized 1.6 times better than in A549 (Fig. 12B).

Next, we examined influence of increased αv integrin expression on the transduction efficiency of HAdV26. The efficiency of HAdV26 transduction was found to be higher in all cell clones with increased αv integrin expression than in the parental A549. The most increased transduction efficiency was observed for the A549-E6 cell clone which expresses 6 times more integrins than A549 cells. HAdV26 transduced A549-D4 and A549-F1 with similar efficiency, 2.7- and 2.4- fold better than A549, respectively (Fig

12C). These data confirm that αv integrin is important for both binding and transduction of HAdV26.

Since it is known that αv integrin most frequently forms heterodimerizes with β1, β3, β5 or β6 subunits, we determined expression of αvβ3, αvβ5, αvβ6 and β1 on the surface of A549-D4, A549-F1 and A549-E6 cells. All three clones have same level of expression of the αvβ5 heterodimer (Fig. 11C) and the β1 integrin subunit (Fig. 11D) as the parental A549 cells. Neither A549 nor A549-D4, A549-F1 and A549-E6 showed expression of αvβ6 integrin (data not shown). However clone A549-E6 was found to have strikingly higher expression of αvβ3 integrin than A549, A549-D4 or A549-F1 (Fig. 11B). Since clones A549-D4, A549-F1 and A549-E6 have comparable expression of αvβ5 (Fig. 11C) and β1 (Fig. 11D) as A549, but show increased transduction efficiency with HAdV26 we conclude that the expression of αvβ5 and β1 is not critical for HAdV26 binding or transduction. Based on the data with respect to the greatly increased expression of αvβ3 integrin in the A549-E6 clone, we assume that αvβ3 integrin is the molecule responsible for increased transduction efficiency of HAdV26 in this cell clone. To further confirm this hypothesis, we stably transfected A549 cells with β3 integrin subunit expression plasmid and isolated 3 clones with increased expression of αvβ3 integrin: A549-B1, A549-B3 and A549-B4 (Fig. 13B). Even though all 3 clones with increased β3 integrin subunit expression, A549-B1, A549-B3 and A549-B4, have increased expression of αvβ3 integrin they do not show increased binding (Fig. 14A) or internalization (Fig. 14B) with HAdV26, which is different than what was observed with A549-E6. Nevertheless, the transduction efficiency of HAdV26 is increased in all three clones A549-B1, A549-B3 and A549-B4, 1.6-, 3.7- and 5.4- fold respectively (Fig. 14C). This increased

transduction matched the increased expression of αvβ3 integrin. Stable transfection of the β3 integrin subunit in A549 cells did not change expression of αvβ5 (Fig. 13C) or β1 (Fig. 13B), further confirming that their presence is not crucial for HAdV26 transduction efficiency. We obtained similar results in HEp2 cell clones with *de novo* expression of αvβ3 integrin (29) where high expression of αvβ3 integrin caused increased transduction efficiency of HAdV26 (data not shown). Importance of αvβ3 integrin in transduction of A549 cells was also confirmed by preincubating cells with vitronectin and RGD peptide, known ligand for αvβ3 integrin, prior infection with HAdV26. Incubation with both vitronectin and RGD peptide decreased transduction efficiency of HAdV26 in A549 cells (Fig. 15). Based on our results obtained in A549-E6, A549-B3 and A549-B4 clones we conclude that αvβ3 integrin is required for efficient transduction of epithelial cells with HAdV26.

Since internalization of HAdV26 in A549 clones with increased expression of αvβ3 integrin measured by qPCR did not completely correspond to increased transduction in those cell clones, we decided to study intracellular trafficking of HAdV26 in A549, A549-B4 and A549-E6 by confocal microscopy. We fluorescently labeled HAdV26 and observed its localization in the cells 2h post infection (Fig. 16A). In both A549-B4 and A549-E6 cell clones the average amount of HAdV26 per cell was higher than in parental A549 cells, i.e., 22 viruses per cell in A549 versus 40 and 82 viruses per cell in A549-B4 and A549-E6 respectively (Fig. 16B). Based on these data we conclude that overexpression of αvβ3 integrin in A549 cells allows both better internalization and transduction efficiency of HAdV26.

HAdV26 shows co-localization with αvβ3 integrin. To get further insight into the interaction between HAdV26 and αvβ3 integrin we asked if HAdV26 co-localizes with αvβ3 integrin in A549-E6, the cell clone with the highest expression of αvβ3 integrin. Fluorescently labeled HAdV26 was incubated with A549-E6 on ice for 30 minutes and then transferred to 37°C for one minute to trigger internalization. Immediately afterwards, cells were transferred to ice to stop internalization. We assumed that at this time point we should be able to capture co-localization between HAdV26 and αvβ3 integrin if there is any. About 80% of the HAdV26 virions detected in this condition, were found to co-localize either partially or completely with αvβ3 integrin indicating that HAdV26 can use αvβ3 integrin as a receptor for infecting epithelial cells (Fig. 17).

DISCUSSION

In this study we found that HAdV26 uses αvβ3 integrin as a receptor for infecting epithelial cells. Until now, molecules that can serve as receptors for HAdV26 infection have been mostly studied in cells circulating in blood. It has been shown that HAdV26 uses CD46 as a receptor for cell entry in human peripheral blood mononuclear cells (25) and B cells (27). There are studies that show that other known adenovirus receptors like CAR and αv integrins could be involved in HAdV26 infection (26). So far the only study regarding HAdV26 receptor in epithelial cells was done on HEp3 cells where it was shown that the RGD-4C peptide partially inhibited oncolysis by species D viruses HAdV17, HAdV24, HAdV26, and HAdV48 indicating involvement of αv integrins in species D adenoviruses infection (27). Therefore, in this study we investigated the role of the above mentioned molecules for HAdV26 infection of human epithelial cells.

We compared the transduction efficiency of HAdV26 on A549 and SK-OV-3 cell lines and observed very low transduction efficiency of HAdV26 on A549 and higher transduction efficiency of HAdV26 on SK-OV-3, suggesting that these two cell lines differ in the expression of the HAdV26 receptor. We also observed low binding and internalization of HAdV26 in A549 cells, presumably reflecting inadequate amounts of HAdV26 receptor for efficient infection. We found that A549 cells express CAR, CD46 and αv integrins, while SK-OV-3 cells show expression only of CD46 and αv integrins, and have little or no CAR on their surface. Expression of CD46 and αv integrins, namely αvβ3 and αvβ5 known to be involved in binding RGD sequence from adenovirus penton, are different in these two cell lines. To investigate the role of above mentioned adenovirus receptors and determine their importance for HAdV26 infection, we downregulated CAR, CD46 and/or αv integrins and studied how this downregulation influenced HAdV26 transduction efficiency. As reference viruses we used HAdV5 which uses CAR for initial binding and αv integrins as co-receptors, and HAdV35 as a representative of CD46 binding virus. Additionally, we used HAdV26F35, a chimeric HAdV26 vector pseudotyped with the HAdV35 fiber, which we assumed uses CD46 for cell binding. Confirmation of this assumption came from our own observation that incubation of A549 with HAdV35 and HAdV26F35 for 4 hours on 37°C resulted in a significant decrease of CD46 on the cell surface indicating that CD46 is internalized together with these viruses upon binding (data not shown), indirectly confirming that HAdV26F35 does indeed binds CD46. However, the transduction efficiency of this chimeric virus might be altered because of the HAdV35 fiber and consequent differences in the engagement between the RGD motif present in HAdV26 penton and integrins.

As expected, downregulation of CAR or αv integrin significantly decreased HAdV5 transduction, while downregulation of CD46 significantly decreased HAdV35 transduction efficiency in both A549 and SK-OV-3, validating our cell model. Downregulation of CAR slightly decreased HAdV26 transduction in A549 cells; however since SK-OV-3 cells have no CAR on their surface, but are transduced better with this virus than A549, we assumed that CAR is not crucial for HAdV26 infection. This assumption is further supported by results obtained in CHO-CAR cells where increased expression of CAR had no influence on HAdV26 transduction efficiency. Downregulation of CAR in A549 cells had very significant negative effect on HAdV35 transduction efficiency which came as a surprise since it is well known that HAdV35 uses CD46 for infecting cells (23). Since blocking CD46 availability with specific antibody had no influence on HAdV35 transduction efficiency and downregulating CAR did not change surface cell expression of CD46, nor changed binding or internalization of this virus, we could assume that some other alteration happened. Since CAR directly interacts with actin (30) and actin dynamics is needed for HAdV35 cytosol localization (31), one could imagine that downregulating CAR might influence HAdV35 infection by modifying actin dynamics and macropinocytosis, process used by HAdV35 for cell entry. To the best of our knowledge there are no published data discussing influence of siCAR on HAdV35 transduction efficiency, however further clarification of this observation is beyond the scope of our work. Unexpectedly, downregulation of CD46 increased transduction efficiency of HAdV26 on A549 and HeLa cells implying that presence of this molecule on A549 cell surface has a negative influence on HAdV26 transduction. We observed the opposite effect in SK-OV-3 cell line where downregulation of CD46 decreased transduction efficiency indicating that in SK-OV-3 cells CD46 contributes to the

transduction efficiency HAdV26. Downregulating CD46 by use of specific siRNA did not change cell surface expression of none of the other investigated receptors, namely CAR, αv integrin, αvβ3 nor αvβ5 integrin, showing that decreased HAdV26 transduction was not due to diminished abundance of cell surface receptor. This observation is consistent, but at this point we cannot explain this phenomenon which seems to be cell specific. Our result is in line with data obtained in peripheral blood mononuclear cells for which was reported that HAdV26 transduction is CD46 dependent (25). Just like SK-OV-3, peripheral blood mononuclear cells are CAR negative (32), suggesting that role of CD46 in HAdV26 transduction efficiency might depend on other molecules present in these cells. Nevertheless, this needs further investigation. Downregulation of αv integrin significantly decreased the transduction efficiency of HAdV26 in A549, SK-OV-3 and HeLa cells indicating that αv integrin is involved in HAdV26 transduction in these cell lines. The same effect was observed in melanoma cell line M21 variants M21L and M21L4. The transduction efficiency of HAdV26 was much higher in M21L4 which are αv integrin positive, than in M21L which are αv integrin negative. Downregulation of αv integrin also decreased the transduction efficiency of HAdV35, albeit much less than HAdV26F35. Since HAdV26F35 possess penton base from HAdV26 it is possible that spatial organization of RGD loop in HAdV26F35 is different from HAdV35, indicating that these two viruses might use αv integrin in a different manner. That αv integrin is necessary for HAdV26 transduction was confirmed also by pre-treating A549 cells with specific blocking antibodies prior to infection. Blocking the surface availability of αv integrin, alone or in combination with both CAR and CD46, significantly decreased transduction efficiency of HAdV26. Blocking CAR or CD46 alone had no effect on HAdV26 infection. At the same time blocking CD46 alone or in combination with CAR or

αv integrin abrogated HAdV26F35 transduction efficiency. Downregulation of αv integrin also decreased binding and internalization of HAdV26 in A549 cells, while downregulating CAR or CD46 had no influence on HAdV26 binding or internalization. This confirms that αv integrin plays an important role in binding and internalization of HAdV26 in A549 cells. All together these data allow us to propose that αv integrin serves as a receptor for HAdV26 in human epithelial cells.

In order to further confirm the role of αv integrin in HAdV26 infection we took a different approach. Instead of downregulating αv integrin we decided to upregulate αv integrin in A549 cells assuming that this would allow for better HAdV26 transduction efficiency. We isolated several stably transfected A549 clones with increased αv integrin expression and measured binding, internalization and transduction efficiency. Increased αv integrin expression in A549 cells resulted in slightly increased binding and internalization of HAdV26 which was followed by significantly increased HAdV26 transduction efficiency in the cell clone with the highest expression of αv integrin. Since it is known that αv integrin exists in interaction with integrin subunits β1, β3, β5, β6 and β8 creating the heterodimers αvβ1, αvβ3, αvβ5, αvβ6 and αvβ8, of which αvβ3 and αvβ5 bind the RGD sequence and serve as co-receptors for adenoviruses, we wanted to determine the status of those heterodimers on the cell surface of A549 resulting from increased expression of the αv integrin subunit. In A549 transfected clones with different levels of expression of the αv integrin subunit, we did not observe changes in the expression of αvβ5 or of β1 (and thus αvβ1). However, in the A549 clone with the highest expression of αv, we detected a large increase in the expression of αvβ3 suggesting that in this clone the higher amount of αv integrin subunit caused augmentation of β3 integrin

subunit expression. We did not detect expression of αvβ6 integrin, and due to the lack of an adequate antibody we did not measure expression of αvβ8 integrin. However, previous reports have stated that A549 cells lack both αvβ6 and αvβ8 integrins (33). Based on these observations we conclude that the molecule responsible for increased HAdV26 transduction efficiency is the αvβ3 integrin. We further corroborated this conclusion by isolating A549 cell clones stably transfected with β3 subunit integrin cDNA. The integrin β3 subunit creates heterodimers only with αv and αIIb subunits. Since the αIIb subunit is a marker of hematopoietic cells (34) we assumed that in A549 cells, the β3 subunit would interact only with the αv subunit resulting in the αvβ3 integrin. We isolated several clones with increased expression of αvβ3 and detected increased HAdV26 transduction efficiency in all of them, in accordance with αvβ3 integrin expression. We also determined the expression levels of αv, αvβ5 and β1 in these clones and verified that increase in αvβ3 integrin did not change expression of any of them, further underlining that the transduction efficiency of HAdV26 depended on the expression of the αvβ3 integrin. Since the promiscuous integrin subunits β1 or αv are synthesized in an excess, the formation of any αβ heterodimer is dependent on the availability of the other subunit, thus formation of αv-containing heterodimers follows hierarchical order. Therefore, the cell surface copy number of for example αvβ3 and αvβ5 integrin is dependent on the amount of β3 and β5 subunits, respectively (29, 35). This can explain why in our A549 cell clones stably overexpressing αv integrin we see upregulation of only αvβ3 and not αvβ5 integrins, i.e. β3 and β5 integrin subunits compete for newly synthesized αv subunit causing difference in expression of αvβ3 and αvβ5 heterodimers.

The discrepancy observed between transduction efficiency and binding/internalization of HAdV26 in A549 clones with increased expression of αvβ3 integrin measured by qPCR could lay in a quite high dissociation constant (Kd) between adenovirus penton and αvβ3 integrin (415 ± 62 nM) (36). Although this Kd refers to HAdV9, we can assume that the Kd value would be similar for HAdV26 because they belong to the same serotype. Since binding assay is performed on ice which does not allow for integrin clustering it is possible that some information could be lost.

Even though the overall structure of the HAdV26 capsid is mostly similar to that of HAdV5, there are some striking differences in structure between these two viruses. One difference with possible implications on αv integrins binding is present in the penton base structure. The sequence alignments between HAdV5 and HAdV26 show that there is a 12-residue deletion at the N terminus and two deletions in the RGD-containing loop in the penton base of HAdV26 relative to species C (15). One could suspect that these changes could render RGD from HAdV26 penton less reachable by αv integrins. HAdV26 has a relatively short fiber with only 8 beta-repeats in the shaft, compared to 22 repeats in the case of HAdV5. This short fiber is assumed to be fairly rigid allowing only limited bending (37). Bending of a long fiber allows easier interaction between RGD from the penton of CAR binding adenoviruses with cell surface integrins which otherwise would not be possible. The RGD binding site on αvβ3 integrin is situated on the top of the integrin subunits and can be reached only when the integrin molecule is activated, i.e. in the extended conformation. According to the current model the length of extended αvβ3 integrin is approximately 20 nm (38). The length of adenovirus fiber with 8 shaft beta-repeats is 11 nm (39). Therefore, αvβ3 integrin in its extended form should be able

to span the distance between the cell surface and HAdV26 penton base and reach RGD peptide, i.e., a rigid fiber should not impair binding of HAdV26 to αvβ3 integrin. In order to corroborate this, further research is needed.

Adenovirus mediated transduction efficiency reflects the sum of adenovirus binding, internalization and intracellular trafficking. Intracellular trafficking is best understood for HAdV5 and includes clathrin-mediated dynamin-dependent endocytosis followed by endosomal escape and cytosolic transport all the way to the nucleus. This entire path is thought to be completed in approximately 90 minutes of infection (40). For HAdV26 there are no detailed reports regarding intracellular trafficking. Here we studied intracellular trafficking of fluorescently labelled HAdV26 in A549 cells and two clones with increased expression of αvβ3 integrin, A549-E6 and A549-B4 120 min post infection. The average number of internalized HAdV26 per cell in in cell clones A549-E6 and A549-B4 was 4 and 2 times higher, respectively, indicating that αvβ3 integrin allows efficient internalization of HAdV26. Additionally, we studied co-localization of HAdV26 and αvβ3 integrin in A549-E6, the cell clone with the highest expression of αvβ3 integrin, and observed that at a very early time point following binding HAdV26 co-localizes with αvβ3 integrin, confirming that HAdV26 uses αvβ3 integrin as a receptor in epithelial cells. By studying intracellular trafficking of fluorescently labeled HAdV26 in A549 cells we did not observe an accumulation of HAdV26 in the proximity of microtubule-organizing center, as has been described for HAdV5 (41), indicating that HAdV26 might have traffic differently from HAdV5. Further studies are needed in order to learn more about HAdV26 intracellular trafficking.

Data obtained in this study give us new insight into HAdV26 infection pathway confirming that αvβ3 integrin is required for efficient infection of epithelial cells by HAdV26. Recently Casiraghi *et al*. have reported that αvβ3 integrin strongly affects the innate immune response in epithelial cells. They showed that αvβ3 integrin greatly increased the immune response elicited by herpes simplex virus which had previously been shown to bind αvβ3 integrin (42). Aforementioned implies that HAdV26 interaction with αvβ3 integrin might also influence the innate immune response in infected cells, therefor it would be interesting to investigate this in more details. Based on our data one could wonder what is the relationship of αvβ3 to the previously reported receptors for this virus, namely CD46 for which has been reported to be involved in binding of the HAdV26 to PBMCs. We would like to point out that PBMCs have almost no expression of αvβ3 and αvβ5 integrin (43) thus αvβ3 integrin is not available as a receptor for HAdV26 in these cells. Results obtained in this study bring us new knowledge regarding HAdV26 receptor usage and should be taken into account when using current or constructing new HAdV26 based vectors for gene transfer and vaccination purposes.

MATERIALS AND METHODS

Cells, viruses, and antibodies. HEK293 (human embryonic kidney: ATCC CRL-1573), A549 (human lung carcinoma: ATCC CCL-185), SK-OV-3 (human ovarian carcinoma: ATCC HTB-77), and HeLa (human cervix adenocarcinoma: ATCC CCL-2) cells were obtained from ATCC Cell Biology Collection and were cultured according to manufacturer's instructions. Adherent CHO-K1 cells (Chinese hamster ovary; ATCC CCL-61) (CAR and CD46 negative) and CHO-CAR cells (CHO cells transfected to stably

express human CAR) were kind gift from George Santis, King's College London School of Medicine, London, UK. CHO-BC1 (CHO cells stably transfected to express CD46) were previously described (44). Melanoma M21 variants M21L and M21L4 (45) were kindly supplied by Prof. Urs Greber, University of Zurich, Switzerland. Replication-incompetent recombinant adenoviral vectors based on adenovirus type 5, 26 and 35 were previously constructed (20, 46). Viruses were propagated on HEK293 cells and purified by CsCl gradients. They carry either the enhanced green fluorescent protein or luciferase gene driven by the CMV promoter as a reporter gene. Antibodies used for flow cytometry, immunohistochemistry, co-localization, and infection competition analyses were the following: anti-CAR (RcmB) from Merck Millipore, anti-CD46 (MEM-258) from Thermo Fisher Scientific, anti-αvβ3 integrin (LM609) from Merck Millipore, anti-αvβ5 integrin (P1F6) from Merck Millipore,anti-αv (272-17E6) from Merck Millipore, anti-β1 (JB1A) from Merck Millipore, anti-αvβ6 integrin (E7P6) from Merck Millipore and FITC goat anti-mouse IgG, cat # 554001 from BD Pharmingen.

Adenovirus infection assay. Adherent cells were incubated with viruses at 37°C and transduction efficiency was measured 48h after infection by assaying for luciferase activity (Promega, Southhampton, UK) or by flow cytometry in case of the GFP reporter. For the measurement of transduction efficiency in the presence of function-blocking antibodies cells were incubated with antibodies at a final concentration of 20 µg/mL for 1 hour on ice prior to incubation with viruses for 1h on ice. Cells were then rinsed and transferred to 37°C. Transduction efficiency was measured 48 h after infection. For the measurement of transduction efficiency in the presence of vitronectin or RGD peptide cells were incubated with vitronectin or RGD peptide for 1 hour on ice prior to incubation

with viruses for 1h on ice. Cells were then rinsed and transferred to 37°C. Transduction efficiency was measured 48 h after infection.For the measurement of transduction efficiency after downregulating specific receptors using siRNA, cells were transfected with the specific siRNA, (50 nM final concentration), and infected with adenoviruses 48 h later. Transduction efficiency was measured 48 h after infection.

Adenovirus Labeling. After purification by banding in CsCl and dialysis against PBS buffer, adenovirus particles were incubated with a 20-fold excess of chemically reactive Alexa488-TFP (Molecular Probes, USA) for 2 hours at room temperature in PBS buffer, pH 7.2. The labeled viral particles were then purified from excess dye by dialysis using Zeba Spin Desalting columns (Pierce). The transduction efficiency of the modified vector was analyzed by transduction assay in HEK-293 cells. Alexa488-TFP labeling did not alter the transduction efficiency of labeled viruses.

siRNA experiments. To downregulate specific receptors, we used the following Silencer Select Predesigned siRNAs: CAR siRNA ID s3774, CD46 siRNA ID s8604, αv integrin siRNA ID s7570, scrambled siRNA #1, catalog No. 4390844, all from Thermo Fisher Scientific. Cells were transfected at a confluency of 30–50% using Lipofectamine RNAiMAX reagent (Invitrogen) according to the manufacturer's protocol. Efficiency of silencing was verified 48 h after transfection by flow cytometry.

Flow Cytometry. Flow cytometry was used to analyze expression of CAR, CD46, αv integrin subunit, β1 integrin subunit and integrin heterodimers αvβ3, αvβ5 and αvβ6. Briefly, adherent cells were grown in tissue culture dishes, detached and washed twice with PBS. Subsequently cells were incubated on ice with the specific primary antibodies that recognize: CAR, CD46, αv integrin, β1 integrin, αvβ3 integrin, αvβ5 integrin and

αvβ6 integrin. The binding of unlabeled primary antibodies was revealed by using FITC-conjugated anti-mouse Ig as a secondary reagent.

Binding and internalization. Adherent cells were grown in multi-well 6 culture dishes until 80% confluency. Adenoviruses, 1000 physical particles per cell, were added to cells and incubated for 1h on ice. To measure binding, unbound viruses were removed by washing the cells twice with cold trypsin and twice with cold PBS. Cells were then harvested with a cell scraper and pelleted by centrifugation. To measure internalization, unbound viruses were removed, warm growth medium was added and cells were transferred to 37ºC allowing viruses to enter the cells. After incubation at 37°C for 1h, cells were washed twice with warm trypsin, dispersed, and pelleted by centrifugation. Total DNA (cellular plus viral) was extracted using commercially available materials (DNeasy Kit, Qiagen) and used to quantify viral DNA. To measure the extent of viral attachment or internalization, viral DNA was quantified by qPCR on 100 ng of total DNA. Viral DNA was detected by qPCR using primers for the CMV sequence (CMV Rv: CGATCTGACGGTTCACTAAACG, CMV Fw: TGGGCGGTAGGCGTGTA, CMV probe: TGGGAGGTCTATATAAGC). The amount of viral DNA was normalized using expression of GAPDH.

Isolation of A549 cells stably expressing αv or β3 integrin. Integrin αv-expressing cell clones A549-D4, A549-F1 and A549-E6 were established from A549 cells by stable transfection with the pcDNA2004Neo(-)αv plasmid containing αv integrin subunit cDNA that was purchased from LifeTechnologies. Integrin αvβ3-expressing cell clones A549-B1, A549-B3 and A549-B4 were established from A549 cells by stable transfection with the pcDNA β3 plasmid containing integrin subunit β3 cDNA (kindly provided by E.H.

Danen, Amsterdam, The Netherlands). Plasmid was transfected into A549 cells using Lipofectamine (Invitrogen, La Jolla, CA). The cells were selected in the presence of G418 (0.6 mg/mL) and screened for αv or αvβ3 integrin expression by flow cytometry.

Confocal microscopy. Cells (20000 per coverslip) were seeded in 24-well plates. Two days after labeled adenoviruses were added to cells (50000 pp/cell) and incubated on ice for 30 minutes to allow binding. Subsequently cells were transferred to 37°C for the indicated time. Cells were fixed with 2% paraformaldehyde in PBS for 12 minutes at room temperature. Nuclei were labeled with DAPI. Coverslips were slide mounted by using Fluoromount (Southern Biotech, USA). Confocal laser scanning microscopy analyses were performed using a Leica TCS SP2 AOBS. Observations were made with an x63 objective. Images showing intracellular trafficking of AlexaFluor488 labeled HAdVs are maximum projections of 7 confocal stacks and processed with Leica Application Suite X (LAS X) software platform, Adobe Photoshop CC software (Adobe Systems) and ImageJ. The co-localization analysis was performed using digital images processed with a co-localization plugin in ImageJ.

Statistical analyses. All experiments were performed at least three times (n=3), in duplicates or triplicates, except flow cytometry experiments, which were performed twice (n=2), respectively. The results are expressed as means ± standard deviations and were analyzed either by t test or by two-way analysis of variance. We used GraphPad Prism software. All P values of <0.05 were considered statistically significant.

ACKNOWLEDGMENTS

This investigation was supported by Croatian Science Foundation Installation Research Project UIP-2014-09-3912 and Marie Curie Initial Training Network “ADVance” Grant FP7-290002.

CONFLICTS OF INTEREST

T. U., J. V. and J. C. are employees of Janssen Vaccines and Prevention BV, Leiden, The Netherlands.

REFERENCES

1. **Mangel WF, San Martin C.** 2014. Structure, Function and Dynamics in Adenovirus Maturation. Viruses-Basel **6:**4536-4570.
2. **Nemerow GR, Stewart PL, Reddy VS.** 2012. Structure of human adenovirus. Curr Opin Virol **2:**115-121.
3. **Zhang C, Zhou DM.** 2016. Adenoviral vector-based strategies against infectious disease and cancer. Hum Vacc Immunother **12:**2064-2074.
4. **Hendrickx R, Stichling N, Koelen J, Kuryk L, Lipiec A, Greber UF.** 2014. Innate Immunity to Adenovirus. Hum Gene Ther **25:**265-284.
5. **Hartman ZC, Kiang A, Everett RS, Serra D, Yang XY, Clay TM, Amalfitano A.** 2007. Adenovirus infection triggers a rapid, MyD88-regulated transcriptome response critical to acute-phase and adaptive immune responses in vivo. J Virol **81:**1796-1812.
6. **Madisch I, Harste G, Pommer H, Heim A.** 2005. Phylogenetic analysis of the main neutralization and hemagglutination determinants of all human adenovirus prototypes as a basis for molecular classification and taxonomy. J Virol **79:**15265-15276.
7. **Walsh MP, Seto J, Liu EB, Dehghan S, Hudson NR, Lukashev AN, Ivanova O, Chodosh J, Dyer DW, Jones MS, Seto D.** 2011. Computational Analysis of Two Species C Human Adenoviruses Provides Evidence of a Novel Virus. J Clin Microbiol **49:**3482-3490.
8. **Robinson CM, Singh G, Henquell C, Walsh MP, Peigue-Lafeuille H, Seto D, Jones MS, Dyer DW, Chodosh J.** 2011. Computational analysis and identification of an emergent human adenovirus pathogen implicated in a respiratory fatality. Virology **409:**141-147.
9. **Meier O, Greber UF.** 2003. Adenovirus endocytosis. J Gene Med **5:**451-462.
10. **Nwanegbo E, Vardas E, Gao WT, Whittle H, Sun HJ, Rowe D, Robbins PD, Gambotto A.** 2004. Prevalence of neutralizing antibodies to adenoviral serotypes 5 and 35 in the adult populations of The Gambia, South Africa, and the United States. Clin Diagn Lab Immun **11:**351-357.
11. **Holterman L, Vogels R, van der Vlugt R, Sieuwerts M, Grimbergen J, Kaspers J, Geelen E, van der Helm E, Lemckert A, Gillissen G, Verhaagh S, Custers J, Zuijdgeest D, Berkhout B, Bakker M, Quax P, Goudsmit J, Havenga M.** 2004. Novel replication-incompetent vector derived from adenovirus type 11 (Ad11) for vaccination and gene therapy: Low seroprevalence and non-cross-reactivity with Ad5. J Virol **78:**13207-13215.

12. **Roy S, Medina-Jaszek A, Wilson MJ, Sandhu A, Calcedo R, Lin J, Wilson JM.** 2011. Creation of a panel of vectors based on ape adenovirus isolates. J Gene Med **13:**17-25.
13. **Ewer K, Rampling T, Venkatraman N, Bowyer G, Wright D, Lambe T, Imoukhuede EB, Payne R, Fehling SK, Strecker T, Biedenkopf N, Krahling V, Tully CM, Edwards NJ, Bentley EM, Samuel D, Labbe G, Jin J, Gibani M, Minhinnick A, Wilkie M, Poulton I, Lella N, Roberts R, Hartnell F, Bliss C, Sierra-Davidson K, Powlson J, Berrie E, Tedder R, Roman F, De Ryck I, Nicosia A, Sullivan NJ, Stanley DA, Mbaya OT, Ledgerwood JE, Schwartz RM, Siani L, Colloca S, Folgori A, Di Marco S, Cortese R, Wright E, Becker S, Graham BS, Koup RA, Levine MM, Volkmann A, Chaplin P, Pollard AJ, Draper SJ, Ballou WR, Lawrie A, Gilbert SC, Hill AV.** 2016. A Monovalent Chimpanzee Adenovirus Ebola Vaccine Boosted with MVA. The New England journal of medicine **374:**1635-1646.
14. **Davison AJ, Benko M, Harrach B.** 2003. Genetic content and evolution of adenoviruses. J Gen Virol **84:**2895-2908.
15. **Yu XD, Veesler D, Campbell MG, Barry ME, Asturias FJ, Barry MA, Reddy VS.** 2017. Cryo-EM structure of human adenovirus D26 reveals the conservation of structural organization among human adenoviruses. Sci Adv **3**.
16. **Waddington SN, Mcvey JH, Bhella D, Parker AL, Barker K, Atoda H, Pink R, Buckley SMK, Greig JA, Denby L, Custers J, Morita T, Francischetti IMB, Monteiro RQ, Barouch DH, van Rooijen N, Napoli C, Hlavenga MJE, Nicklin SA, Baker AH.** 2008. Adenovirus serotype 5 hexon mediates liver gene transfer. Cell **132:**397-409.
17. **Milligan ID, Gibani MM, Sewell R, Clutterbuck EA, Campbell D, Plested E, Nuthall E, Voysey M, Silva-Reyes L, McElrath MJ, De Rosa SC, Frahm N, Cohen KW, Shukarev G, Orzabal N, van Duijnhoven W, Truyers C, Bachmayer N, Splinter D, Samy N, Pau MG, Schuitemaker H, Luhn K, Callendret B, Van Hoof J, Douoguih M, Ewer K, Angus B, Pollard AJ, Snape MD.** 2016. Safety and Immunogenicity of Novel Adenovirus Type 26-and Modified Vaccinia Ankara-Vectored Ebola Vaccines A Randomized Clinical Trial. Jama-J Am Med Assoc **315:**1610-1623.
18. **Baden LR, Walsh SR, Seaman MS, Tucker RP, Krause KH, Patel A, Johnson JA, Kleinjan J, Yanosick KE, Perry J, Zablowsky E, Abbink P, Peter L, Iampietro MJ, Cheung A, Pau MG, Weijtens M, Goudsmit J, Swann E, Wolff M, Loblein H, Dolin R, Barouch DH.** 2013. First-in-Human Evaluation of the Safety and Immunogenicity of a Recombinant Adenovirus Serotype 26 HIV-1 Env Vaccine (IPCAVD 001). J Infect Dis **207:**240-247.
19. **Barouch DH, Tomaka FL, Wegmann F, Stieh DJ, Alter G, Robb ML, Michae NL, Peter L, Nkolola JP, Borducchi EN, Chandrashekar A, Jetton D, Stephenson KE, Li WJ, Korber B, Tomaras GD, Montefiori DC, Gray G, Frahm N, McElrath MJ, Baden L, Johnson J, Hotter J, Swann E, Karita E, Kibuuka H, Mpendo J, Garrett N, Mngadi K, Chinyenze K, Priddy F, Lazarus E, Laher F, Nitayapan S, Pitisuttithum P, Bart S, Campbell T, Feldman R, Lucksinger G, Borremans C, Callewaert K, Roten R, Sadoff J, Scheppler L, Weijtens M, Feddes-de Boer K, van Manen D, Vreugdenhil J, Zahn R, Lavreys L, Nijs S, Tolboom J, Hendriks J, Euler Z, Pau MG, Schuitemaker H.** 2018. Evaluation of a mosaic HIV-1 vaccine in a multicentre, randomised, double-blind, placebo-controlled, phase 1/2a clinical trial (APPROACH) and in rhesus monkeys (NHP 13-19). Lancet **392:**232-243.
20. **Abbink P, Lemckert AAC, Ewald BA, Lynch DM, Denholtz M, Smits S, Holterman L, Damen I, Vogels R, Thorner AR, O'Brien KL, Carville A, Mansfield KG, Goudsmit J, Havenga MJE, Barouch DH.** 2007. Comparative seroprevalence and immunogenicity of six rare serotype recombinant adenovirus vaccine vectors from subgroups B and D. J Virol **81:**4654-4663.
21. **Arnberg N.** 2012. Adenovirus receptors: implications for targeting of viral vectors. Trends Pharmacol Sci **33:**442-448.

22. **Bergelson JM, Cunningham JA, Droguett G, KurtJones EA, Krithivas A, Hong JS, Horwitz MS, Crowell RL, Finberg RW.** 1997. Isolation of a common receptor for coxsackie B viruses and adenoviruses 2 and 5. Science **275:**1320-1323.
23. **Gaggar A, Shayakhmetov DM, Lieber A.** 2003. CD46 is a cellular receptor for group B adenoviruses. Nat Med **9:**1408-1412.
24. **Nemerow GR, Stewart PL.** 1999. Role of alpha(v) integrins in adenovirus cell entry and gene delivery. Microbiology and molecular biology reviews : MMBR **63:**725-734.
25. **Li HL, Rhee EG, Masek-Hammerman K, Teigler JE, Abbink P, Barouch DH.** 2012. Adenovirus Serotype 26 Utilizes CD46 as a Primary Cellular Receptor and Only Transiently Activates T Lymphocytes following Vaccination of Rhesus Monkeys. J Virol **86:**10862-10865.
26. **Chen H, Xiang ZQ, Li Y, Kurupati RK, Jia B, Bian A, Zhou DM, Hutnick N, Yuan S, Gray C, Serwanga J, Auma B, Kaleebu P, Zhou X, Betts MR, Ertl HCJ.** 2010. Adenovirus-Based Vaccines: Comparison of Vectors from Three Species of Adenoviridae. J Virol **84:**10522-10532.
27. **Chen CY, Senac JS, Weaver EA, May SM, Jelinek DF, Greipp P, Witzig T, Barry MA.** 2011. Species D Adenoviruses as Oncolytics against B-cell Cancers. Clin Cancer Res **17:**6712-6722.
28. **Stichling N, Suomalainen M, Flatt JW, Schmid M, Pacesa M, Hemmi S, Jungraithmayr W, Maler MD, Freudenberg MA, Pluckthun A, May T, Koster M, Fejer G, Greber UF.** 2018. Lung macrophage scavenger receptor SR-A6 (MARCO) is an adenovirus type-specific virus entry receptor. PLoS pathogens **14:**e1006914.
29. **Ambriovic-Ristov A, Gabrilovac J, Cimbora-Zovko T, Osmak M.** 2004. Increased adenoviral transduction efficacy in human laryngeal carcinoma cells resistant to cisplatin is associated with increased expression of integrin alphavbeta3 and coxsackie adenovirus receptor. International journal of cancer **110:**660-667.
30. **Huang KC, Yasruel Z, Guerin C, Holland PC, Nalbantoglu J.** 2007. Interaction of the Coxsackie and adenovirus receptor (CAR) with the cytoskeleton: Binding to actin. Febs Lett **581:**2702-2708.
31. **Kalin S, Amstutz B, Gastaldelli M, Wolfrum N, Boucke K, Havenga M, DiGennaro F, Liska N, Hemmi S, Greber UF.** 2010. Macropinocytotic Uptake and Infection of Human Epithelial Cells with Species B2 Adenovirus Type 35. J Virol **84:**5336-5350.
32. **Havenga MJ, Lemckert AA, Ophorst OJ, van Meijer M, Germeraad WT, Grimbergen J, van Den Doel MA, Vogels R, van Deutekom J, Janson AA, de Bruijn JD, Uytdehaag F, Quax PH, Logtenberg T, Mehtali M, Bout A.** 2002. Exploiting the natural diversity in adenovirus tropism for therapy and prevention of disease. J Virol **76:**4612-4620.
33. **Goodman SL, Grote HJ, Wilm C.** 2012. Matched rabbit monoclonal antibodies against alpha v-series integrins reveal a novel alpha v beta 3-LIBS epitope, and permit routine staining of archival paraffin samples of human tumors. Biol Open **1:**329-340.
34. **Durrant TN, van den Bosch MT, Hers I.** 2017. Integrin alphaIIbbeta3 outside-in signaling. Blood **130:**1607-1619.
35. **Koistinen P, Heino J.** 2002. The selective regulation of alpha(v)beta(1) integrin expression is based on the hierarchical formation of alpha(v)-containing heterodimers. J Biol Chem **277:**24835-24841.
36. **Veesler D, Cupelli K, Burger M, Graber P, Stehle T, Johnson JE.** 2014. Single-particle EM reveals plasticity of interactions between the adenovirus penton base and integrin alpha(V)beta(3). P Natl Acad Sci USA **111:**8815-8819.
37. **Wu E, Pache L, Von Seggern DJ, Mullen TM, Mikyas Y, Stewart PL, Nemerow GR.** 2003. Flexibility of the adenovirus fiber is required for efficient receptor interaction. J Virol **77:**7225-7235.
38. **Takagi J, Petre BM, Walz T, Springer TA.** 2002. Global conformational rearrangements in integrin extracellular domains in outside-in and inside-out signaling. Cell **110:**599-611.

39. **Shayakhmetov DM, Lieber A.** 2000. Dependence of adenovirus infectivity on length of the fiber shaft domain. J Virol **74:**10274-10286.
40. **Luisoni S, Greber UF.** 2016. 2 - Biology of Adenovirus Cell Entry: Receptors, Pathways, Mechanisms A2 - Curiel, David T, p. 27-58, Adenoviral Vectors for Gene Therapy (Second Edition). Academic Press, San Diego.
41. **Bailey CJ, Crystal RG, Leopold PL.** 2003. Association of adenovirus with the microtubule organizing center. J Virol **77:**13275-13287.
42. **Casiraghi C, Gianni T, Campadelli-Fiume G.** 2016. alpha v beta 3 Integrin Boosts the Innate Immune Response Elicited in Epithelial Cells through Plasma Membrane and Endosomal Toll-Like Receptors. J Virol **90:**4243-4248.
43. **Huang SA, Endo RI, Nemerow GR.** 1995. Up-Regulation of Integrins Alpha-V-Beta-3 and Alpha-V-Beta-5 on Human Monocytes and T-Lymphocytes Facilitates Adenovirus-Mediated Gene Delivery. J Virol **69:**2257-2263.
44. **Trinh HV, Lesage G, Chennamparampil V, Vollenweider B, Burckhardt CJ, Schauer S, Havenga M, Greber UF, Hemmi S.** 2012. Avidity Binding of Human Adenovirus Serotypes 3 and 7 to the Membrane Cofactor CD46 Triggers Infection. J Virol **86:**1623-1637.
45. **Petitclerc E, Stromblad S, von Schalscha TL, Mitjans F, Piulats J, Montgomery AM, Cheresh DA, Brooks PC.** 1999. Integrin alpha(v)beta3 promotes M21 melanoma growth in human skin by regulating tumor cell survival. Cancer Res **59:**2724-2730.
46. **Vogels R, Zuijdgeest D, van Rijnsoever R, Hartkoorn E, Damen I, de Bethune MP, Kostense S, Penders G, Helmus N, Koudstaal W, Cecchini M, Wetterwald A, Sprangers M, Lemckert A, Ophorst O, Koel B, van Meerendonk M, Quax P, Panitti L, Grimbergen J, Bout A, Goudsmit J, Havenga M.** 2003. Replication-deficient human adenovirus type 35 vectors for gene transfer and vaccination: Efficient human cell infection and bypass of preexisting adenovirus immunity. J Virol **77:**8263-8271.

FIGURE LEGENDS

Figure 1. Flow cytometry analysis of known adenovirus receptors, CAR, CD46, αvβ3, αvβ5 and αV integrin, on surface of A549 and SK-OV-3 cells. Cells were detached, incubated with specific antibodies on ice and cell surface expression of CAR, CD46, αv, αvβ3 and αvβ5 integrins was analyzed by flow cytometry. The following antibodies were used in order to detect studied receptors: CAR (RcmB), CD46 (MEM-258), αvβ3 (LM609), αvβ5 (P1F6) and αv (272-17E6). Green and violet colors represent primary antibody staining in the A549 and SK-OV-3 cells, respectively. n=2.

Figure 2. Transduction efficiency of HAdV5, HAdV26, HAdV35 and HAdV26F35 in A549 and SK-OV-3 cells. (A) Comparison in transduction efficiency of HAdV5, HAdV26, HAdV35 and HAdV26F35 in A549 and SK-OV-3 cells. The results are presented as absolute value in RLU per mg of protein. (B) Transduction efficiency of HAdV26 in A549 and SK-OV-3 cells. The results are presented as fold of A549 transduction efficiency. Transduction efficiency was measured by luciferase activity assay 48h after infection.

The results are expressed as means ± standard deviations. *, P<0.05; **, P<0.01; ***, P<0.001. n=3.

Figure 3. Binding and internalization of HAdV5, HAdV26, HAdV35 and HAdV26F35 in A549 and SK-OV-3 cells. Binding and internalization of HAdV5, HAdV26, HAdV35 and HAdV26F35 in A549 cells (A) and in SK-OV-3 cells (B). The results are expressed as fold of control, i.e. value obtained for HAdV5, ± standard deviations. (C) Binding and internalization of HAdV26 in A549 and SK-OV-3 cells. Results are presented as relative to A549, ± standard deviations. For both binding and internalization cells were first incubated with HAdV5, HAdV26, HAdV35 and HAdV26F35 on ice for 1h, moi 1000 vp/cell. To measure binding, unbound viruses were removed by rinsing the cells with cold trypsin and PBS and collected by scraping the cells. For internalization measurement unbound viruses were removed as stated above, cells were transferred to 37ºC and incubated for 1h allowing viruses to enter the cells. Cells were then rinsed twice with warm trypsin, dispersed, and pelleted by centrifugation. For both binding and internalization total DNA (cellular plus viral) was extracted from cells and used for quantification of viral DNA by qPCR using CMV region as a target sequence. *, P<0.05; **, P<0.01; ***, P<0.001. n=3.

Figure 4. Flow cytometry analysis of CAR, CD46 and αv integrin on surface of A549 and SK-OV-3 cells after downregulation by specific siRNA transfection. Cells were transfected with specific siRNA in final concentration 50 nM and 48h later surface expression of CAR, CD46 and αv integrin was determined. The following antibodies were used to detect studied receptors: CAR (RcmB), CD46 (MEM-258) and αv integrin (272-17E6). Results are shown as percentage of the value for the control, i.e. cells transfected with scrambled siRNA. n=2.

Figure 5. Transduction efficiency of HAdV5 (A), HAdV26 (B), HAdV35 (C) and HAdV26F35 (D) in A549 cells after downregulation of CAR, CD46 and/or αv integrin by specific siRNA transfection. Cells were transfected with specific siRNA in final concentration 50 nM and 48h later infected with HAdV5, HAdV26, HAdV35 and HAdV26F35, moi 1000 vp/cell. Transduction efficiency was measured by luciferase activity assay 48h after infection. The results are presented as fold of the control, i.e. cells transfected with scrambled siRNA ± standard deviations. *, P<0.05; **, P<0.01; ***, P<0.001. n=3.

Figure 6. Transduction efficiency of HAdV5, HAdV26, HAdV35 and HAdV26F35 in SK-OV-3 cells after downregulation of CD46 and/or αv integrin by specific siRNA transfection. Cells were transfected with specific siRNA in final concentration 50 nM and 48h later infected with HAdV5, HAdV26, HAdV35 and HAdV26F35, moi 1000 vp/cell. Transduction efficiency was measured by luciferase activity assay 48h after

infection. The results are presented as fold of the control, i.e. cells transfected with scrambled siRNA ± standard deviations. *, P<0.05; **, P<0.01; ***, P<0.001. n=3.

Figure 7. Transduction efficiency of HAdV5, HAdV26, HAdV35 and HAdV26F35 in M21L and M21L4 cells. Cells were infected with HAdV5, HAdV26, HAdV35 and HAdV26F35 at moi 1000 vp/cell. Transduction efficiency was measured by luciferase activity assay 48h after infection. M21L cells are αv integrin negative, and M21L4 are αv integrin positive. The results are presented as absolute value in RLU per mg of protein and shown as means ± standard deviations. *, P<0.05; **, P<0.01; ***, P<0.001. n=2.

Figure 8. Transduction efficiency of HAdV5, HAdV26, HAdV35 and HAdV26F35 in CHO-CAR (A) and CHO-BC1 (B) cells. CHO-CAR cells were incubated with HAdV5 knob (wild type or Y477A) and CHO-BC1 cells with anti-CD46 antibody (MEM258) or IgG1 control on ice for 1h and afterwards infected with HAdV5, HAdV26, HAdV35 and HAdV26F35 at moi 5000 vp/cell. Transduction efficiency was measured by luciferase activity assay 48h after infection. CHO-CAR are CHO cells stably transfected with a plasmid containing CAR cDNA and CHO-R are CHO stably transfected with empty plasmid; CHO-K1 are the normal CHO, and CHO-BC1 are CHO cells stably transfected with a plasmid containing CD46 cDNA. The results are presented as absolute value in RLU per mg of protein and shown as means ± standard deviations. *, P<0.05; **, P<0.01; ***, P<0.001. n=3.

Figure 9. Binding and internalization of HAdV5, HAdV26, HAdV35 and HAdV26F35 in A549 cells after downregulating CAR, CD46 and αv integrins. Cells were transfected with specific siRNA in final concentration 50 nM and 48h later incubated with HAdV5, HAdV26, HAdV35 and HAdV26F35 on ice for 1h, moi 1000 vp/cell. To measure binding, unbound viruses were removed by rinsing the cells with cold trypsin and PBS and collected by scraping the cells. For internalization measurement unbound viruses were removed as stated above, cells were transferred to 37ºC and incubated for 1h allowing viruses to enter the cells. Cells were then rinsed twice with warm trypsin, dispersed, and pelleted by centrifugation. For both binding and internalization total DNA (cellular plus viral) was extracted from cells and used for quantification of viral DNA by qPCR using CMV region as a target sequence. The results are presented as fold of the control, i.e. cells transfected with scrambled siRNA ± standard deviations. *, P<0.05; **, P<0.01; ***, P<0.001. n=3.

Figure 10. Transduction efficiency of HAdV5 (A), HAdV26 (B), HAdV35 (C) and HAdV26F35 (D) in A549 cells after incubation with anti-CAR, anti-CD46 and/or anti-αv integrin blocking antibodies. Cells were first incubated with antibodies on ice for 1h

and afterwards viruses were added. The following antibodies, at final concentration of 20 µg/mL, were used: CAR (RcmB), CD46 (MEM-258), αvβ3 (LM609), αvβ5 (P1F6) and αv (272-17E6). Transduction efficiency was measured by luciferase activity assay 48h after infection. The results are presented as fold of the control, i.e. cells incubated with IgG ± standard deviations. *, P<0.05; **, P<0.01; ***, P<0.001. n=2.

Figure 11. Expression of αv, αvβ3, αvβ5 and β1 integrins in A549 cell clones obtained by stable transfection of A549 cells with the plasmid containing αv integrin subunit cDNA. Cells were detached, incubated with specific antibodies on ice and cell surface expression of αv, αvβ3, αvβ5 and β1 integrins was analyzed by flow cytometry. The following antibodies were used: αvβ3 (LM609), αvβ5 (P1F6) and αv (272-17E6). Representative geomean fluorescence intensities obtained in one of three independent experiments with similar results are shown.

Figure 12. Binding, internalization and transduction efficiency of HAdV26 in A549 cell clones with increased expression of αv integrin. (A) Binding and (B) Internalization of HAdV26 in A549 and A549 cell clones with increased expression of αv integrin: A549-D4, A549-F1 and A549-E6. Cells were incubated with HAdV26 on ice for 1h, moi 1000 vp/cell. To measure binding, unbound viruses were removed by rinsing the cells with cold trypsin and PBS and collected by scraping the cells. For internalization measurement unbound viruses were removed as stated above, cells were transferred to 37ºC and incubated for 1h allowing viruses to enter the cells. Cells were then rinsed twice with warm trypsin, dispersed, and pelleted by centrifugation. For both binding and internalization total DNA (cellular plus viral) was extracted from cells and used for quantification of viral DNA by qPCR using CMV region as a target sequence. The results are expressed as fold of value obtained for A549 ± standard deviations. (C) Transduction efficiency of HAdV26 in A549 and A549 cell clones with increased expression of αv integrin: A549-D4, A549-F1 and A549-E6. Transduction efficiency was measured by flow cytometry 48h after infection. The results are expressed as fold of value obtained for A549 ± standard deviations. *, P<0.05; ** P<0.01; ***, P<0.001. n=3.

Figure 13. Expression of αv, αvβ3, αvβ5 and β1 integrins in A549 cell clones obtained by stable transfection of A549 cells with the plasmid containing β3 integrin subunit cDNA. Cells were detached, incubated with specific antibodies on ice and cell surface expression of αv (A), αvβ3 (B), αvβ5 (C) and β1 (D) integrins was analyzed by flow cytometry. The following antibodies were used: αvβ3 (LM609), αvβ5 (P1F6) and αv (272-17E6). Representative geomean fluorescence intensities obtained in one of three independent experiments with similar results are shown.

Figure 14. Binding, internalization and transduction efficiency of HAdV26 in A549 cell clones with increased expression of β3 integrin. (A) Binding and (B) Internalization of HAdV26 in A549 and A549 cell clones with increased expression of β3

integrin: A549-B1, A549-B3 and A549-B4. Cells were incubated with HAdV26 on ice for 1h, moi 1000 vp/cell. To measure binding, unbound viruses were removed by rinsing the cells with cold trypsin and PBS and collected by scraping the cells. For internalization measurement unbound viruses were removed as stated above, cells were transferred to 37ºC and incubated for 1h allowing viruses to enter the cells. Cells were then rinsed twice with warm trypsin, dispersed, and pelleted by centrifugation. For both binding and internalization total DNA (cellular plus viral) was extracted from cells and used for quantification of viral DNA by qPCR using CMV region as a target sequence. The results are expressed as fold of value obtained for A549 ± standard deviations. (C) Transduction efficiency of HAdV26 in A549 and A549 cell clones with increased expression of β3 integrin: A549-B1, A549-B3 and A549-B4. Transduction efficiency was measured by flow cytometry 48h after infection. The results are expressed as fold of value obtained for A549 ± standard deviations. *, P<0.05; ** P<0.01; ***, P<0.001. n=3.

Figure 15. Transduction efficiency of HAdV26 in A549 cells after incubation with vitronectin and RGD peptide. Cells were first incubated with vitronectin (10 µg/mL) or RGD peptide (15 µg/mL) on ice for 1h and afterwards viruses were added. Transduction efficiency was measured by luciferase activity assay 48h after infection. The results are presented as fold of the control. n=2.

Figure 16. Intracellular trafficking of AlexaFluor488 labeled HAdV26 in A549, A549-B4 and A549-E6 cells. (A) Cells were incubated with AlexaFluor488 labeled HAdV26 (50000 vp/cell), for 2h on 37°C. Non-internalized viruses were rinsed away and cells were fixed with 2% PFA. AlexaFluor488 labeled HAdV26 are presented in green, nuclei stained with DAPI are presented in blue, actin cytoskeleton stained with phalloidin is presented in red. Images shown are maximum projections of confocal stacks. Representative confocal images are shown. Scale bar = 25 µm. (B) Quantification of virus internalization efficiency, expressed as virus number per cell. Error bars represent the means ± standard deviations, and number of cells analyzed is indicated.

Figure 17. Co-localization of AlexaFluor488 labeled HAdV26 with αvβ3 integrin in A549-B6 cells. Cells were incubated with AlexaFluor488 labeled HAdV26 (50000 vp/cell), for 1 min on 37°C, fixed with 2% PFA and subsequently stained for αvβ3 integrin expression (LM609). Representative confocal image of HAdV26 co-localizing with αvβ3 integrin is shown. Grey arrow head indicate co-localization; green arrow head indicates absence of co-localization. Scale bar = 25 µm. Pie chart on the right hand represents quantification of the percentage of co-localized HAdV26 with αvβ3 integrin. Data were collected from 9 cells and 59 viruses that infected the cells.

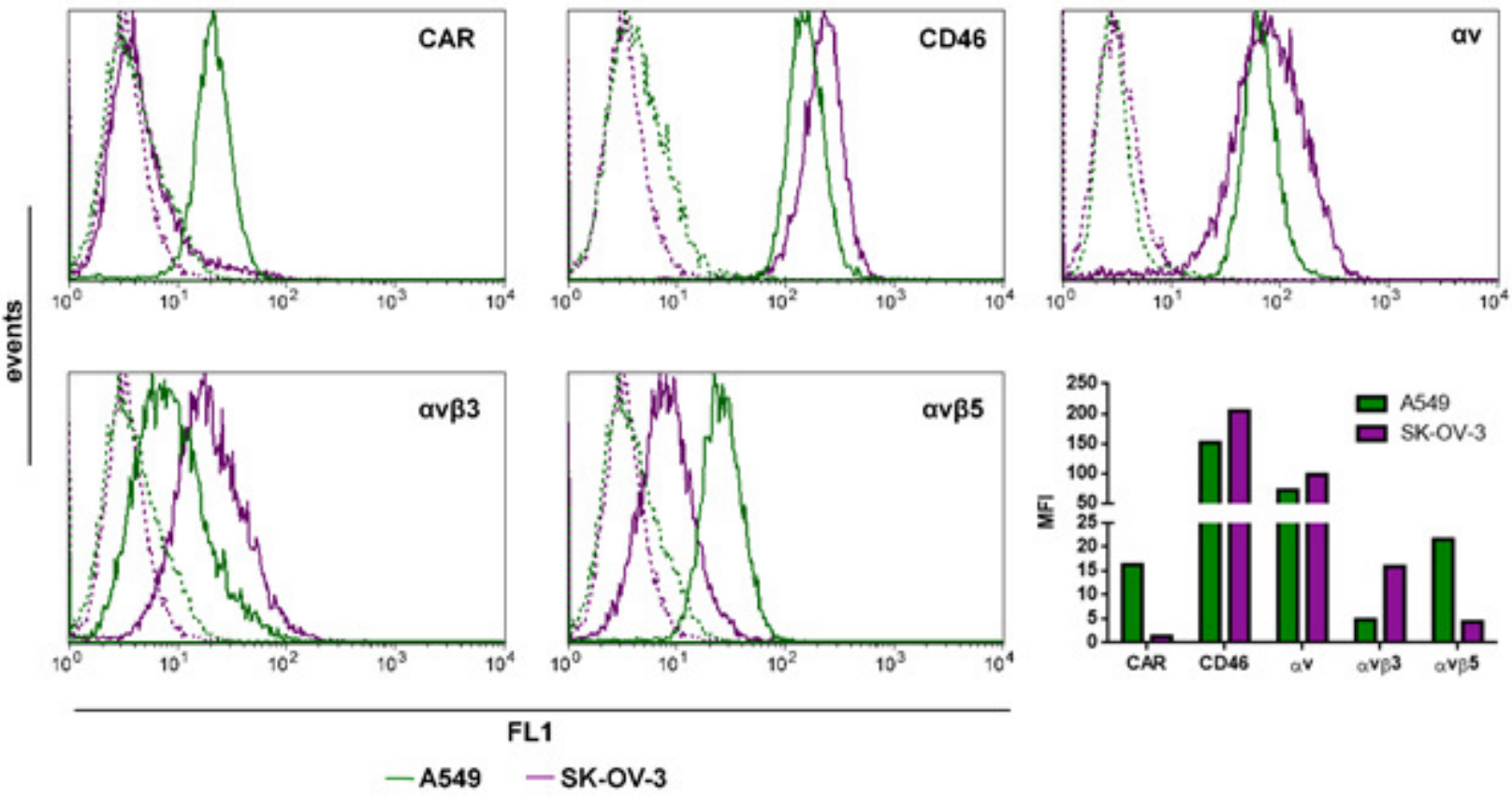
CAR
CD46
αv
αvβ3
αvβ5
events
FL1
A549
SK-OV-3
MFI
250
200
150
100
50
25
20
15
10
5
0
CAR
CD46
αv
αvβ3
αvβ5

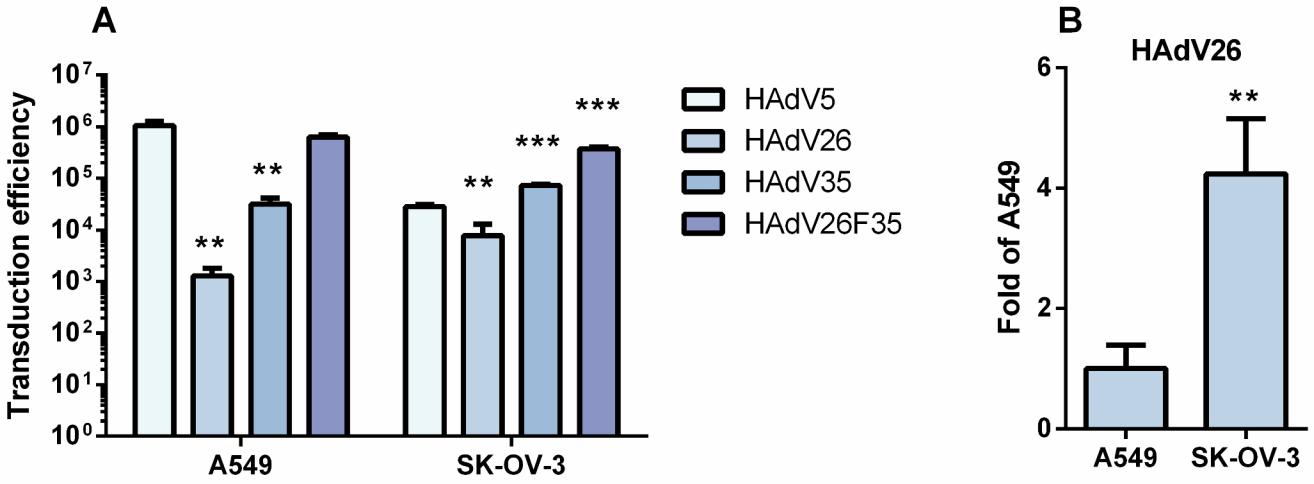
A
Transduction efficiency
10^7
10^6
10^5
10^4
10^3
10^2
10^1
10^0
**
**
**
***
***
A549
SK-OV-3
HAdV5
HAdV26
HAdV35
HAdV26F35
B
HAdV26
Fold of A549
6
4
2
0
**
A549
SK-OV-3

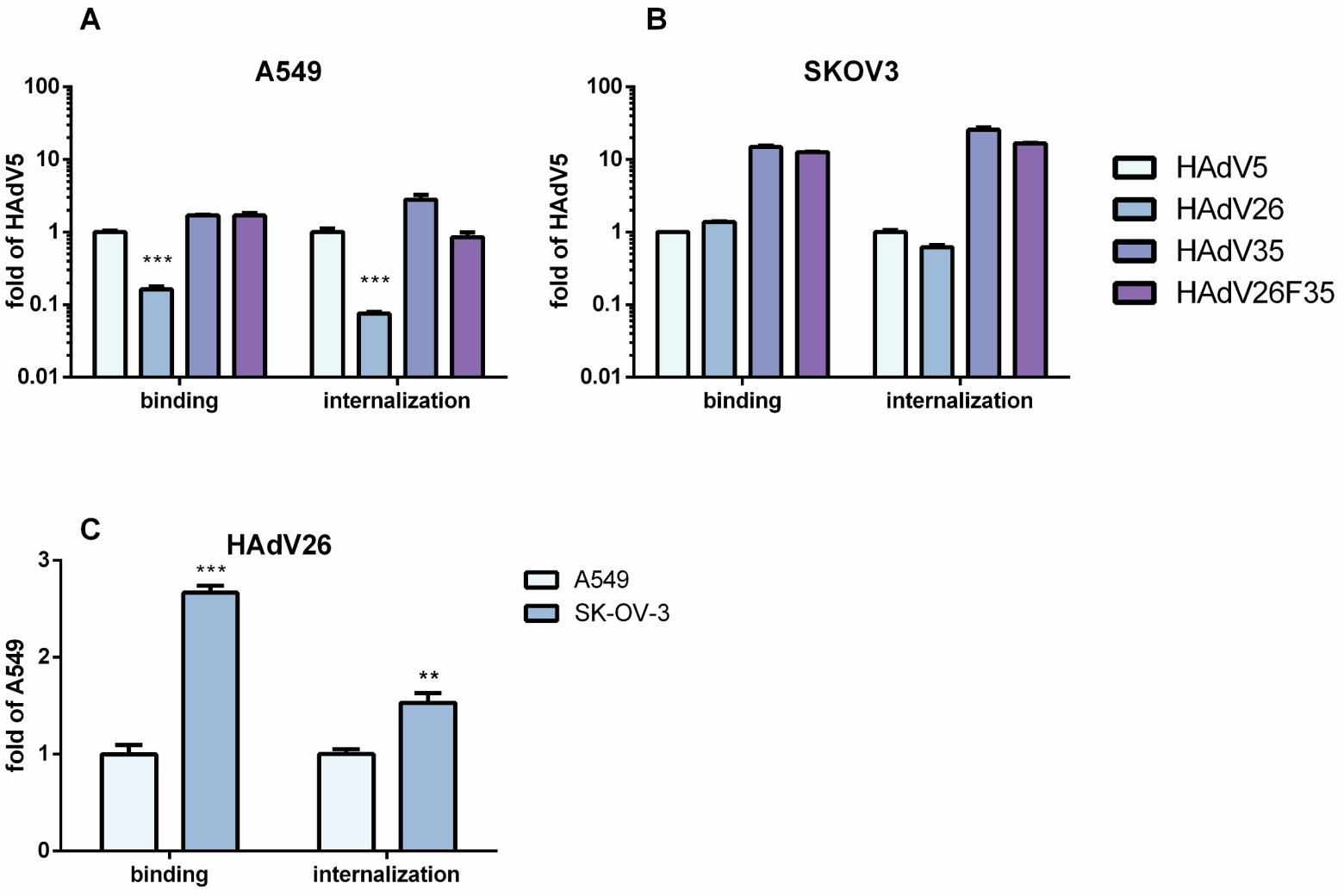
A
A549
100
10
1
0.1
0.01
fold of HAdV5
***
***
binding
internalization
B
SKOV3
100
10
1
0.1
0.01
fold of HAdV5
binding
internalization
HAdV5
HAdV26
HAdV35
HAdV26F35
C
HAdV26
3
2
1
0
fold of A549
***
**
binding
internalization
A549
SK-OV-3

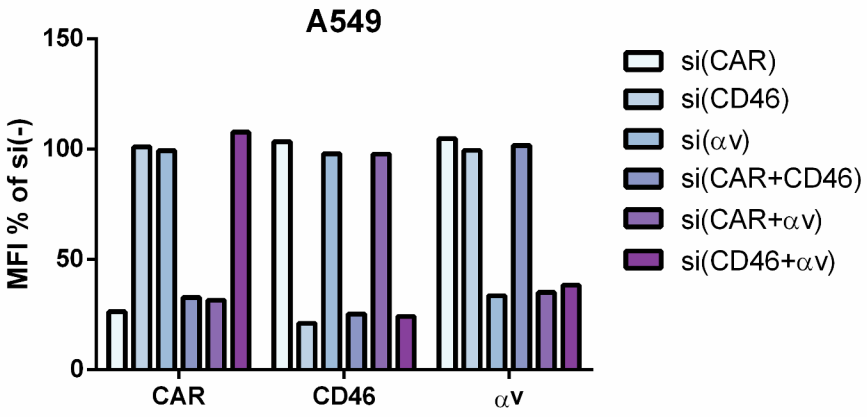
A549
MFI % of si(-)
150
100
50
0
CAR
CD46
αv
si(CAR)
si(CD46)
si(αv)
si(CAR+CD46)
si(CAR+αv)
si(CD46+αv)

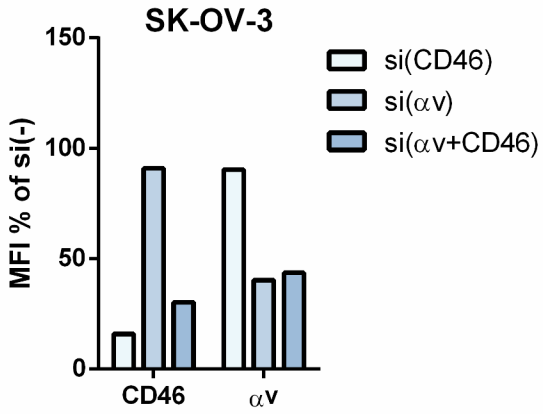
SK-OV-3
MFI % of si(-)
150
100
50
0
CD46
αv
si(CD46)
si(αv)
si(αv+CD46)

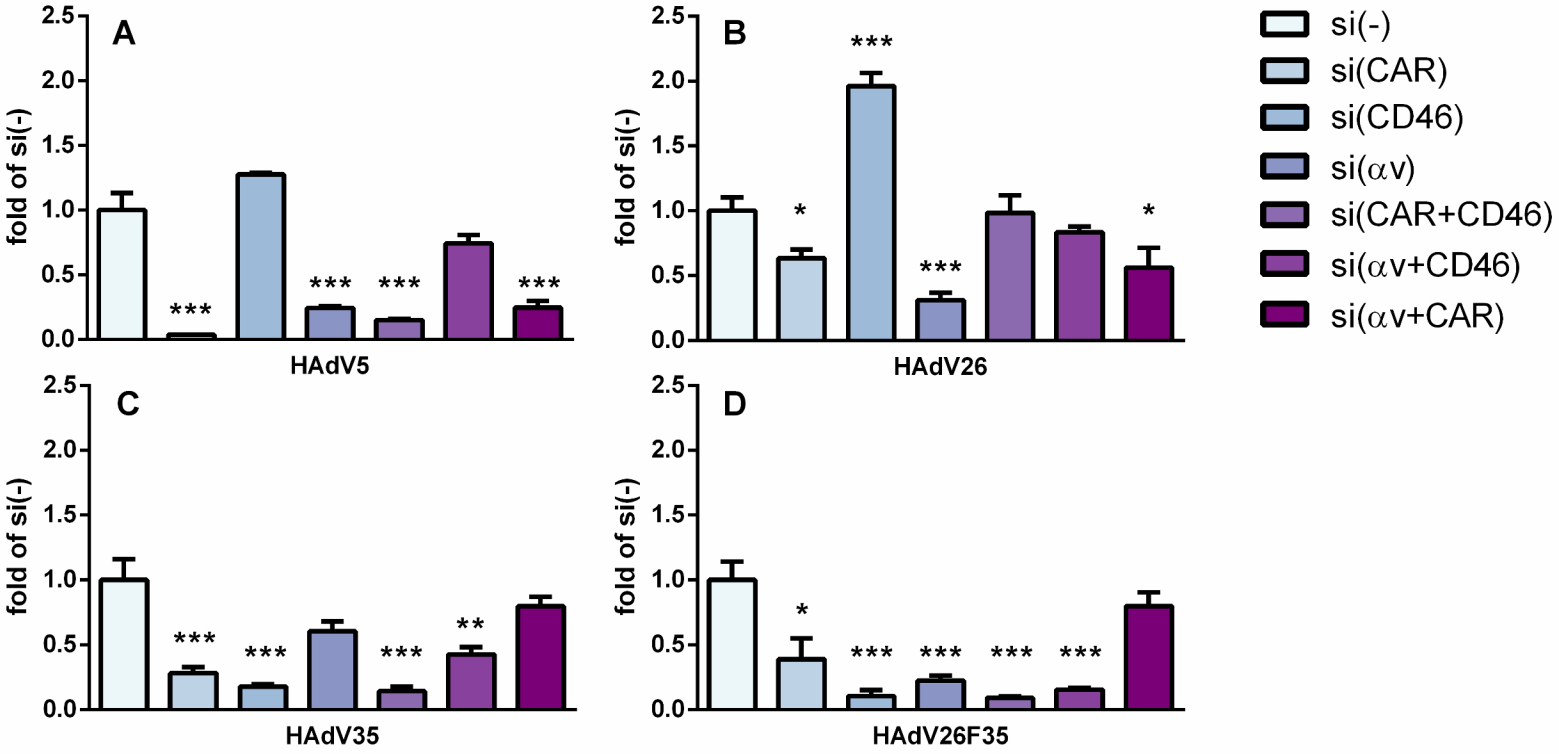
A
B
C
D
fold of si(-)
2.5
2.0
1.5
1.0
0.5
0.0
***
*
**
HAdV5
HAdV26
HAdV35
HAdV26F35
si(-)
si(CAR)
si(CD46)
si(αv)
si(CAR+CD46)
si(αv+CD46)
si(αv+CAR)

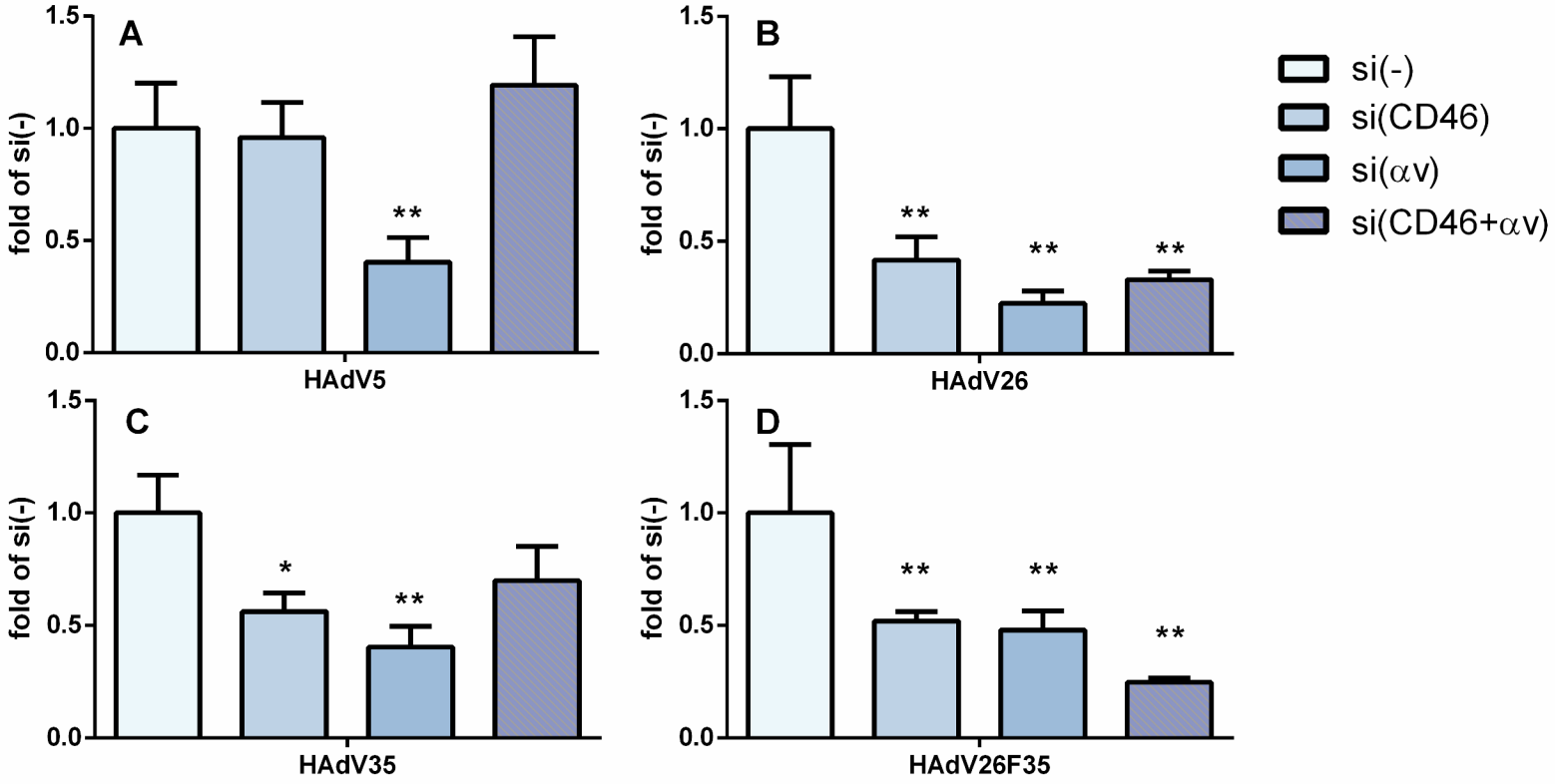
A
B
C
D
fold of si(-)
1.5
1.0
0.5
0.0
**
*
HAdV5
HAdV26
HAdV35
HAdV26F35
si(-)
si(CD46)
si(αv)
si(CD46+αv)

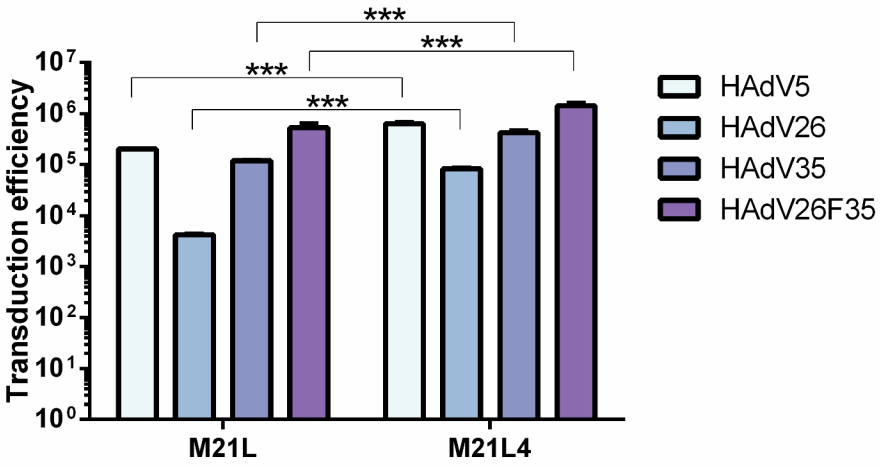
***
***
***
***
Transduction efficiency
10^7
10^6
10^5
10^4
10^3
10^2
10^1
10^0
M21L
M21L4
HAdV5
HAdV26
HAdV35
HAdV26F35

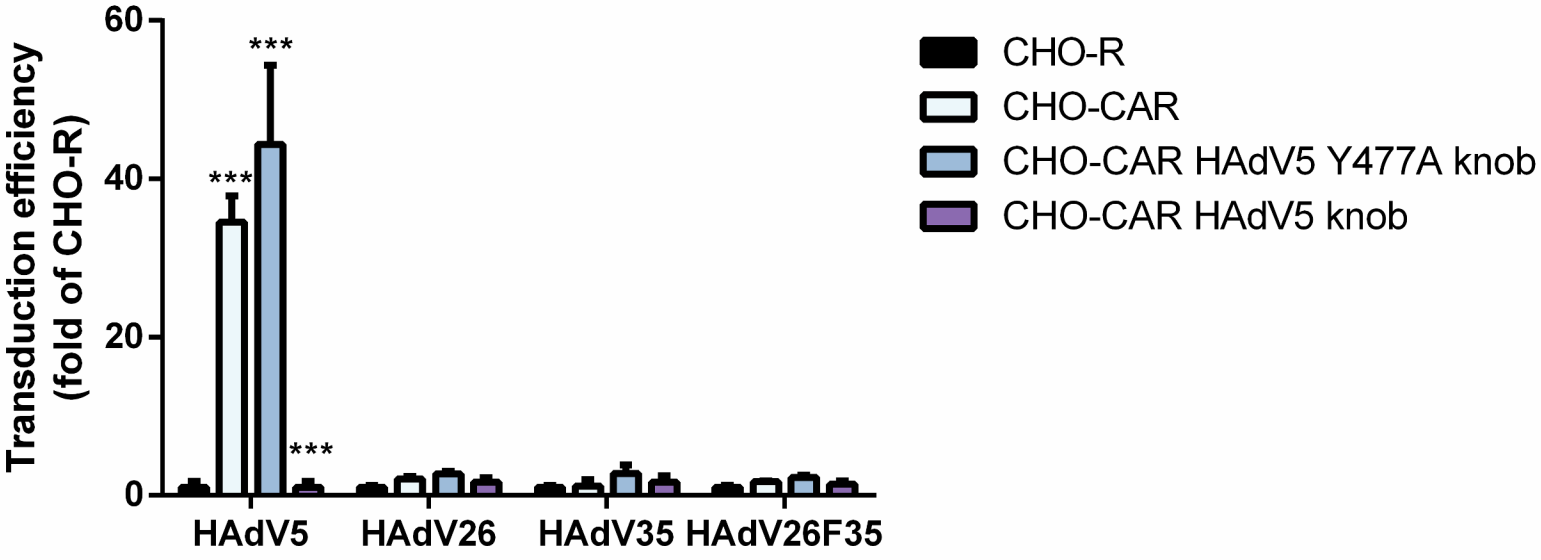
Transduction efficiency
(fold of CHO-R)
60
40
20
0
***
***
***
HAdV5
HAdV26
HAdV35
HAdV26F35
CHO-R
CHO-CAR
CHO-CAR HAdV5 Y477A knob
CHO-CAR HAdV5 knob

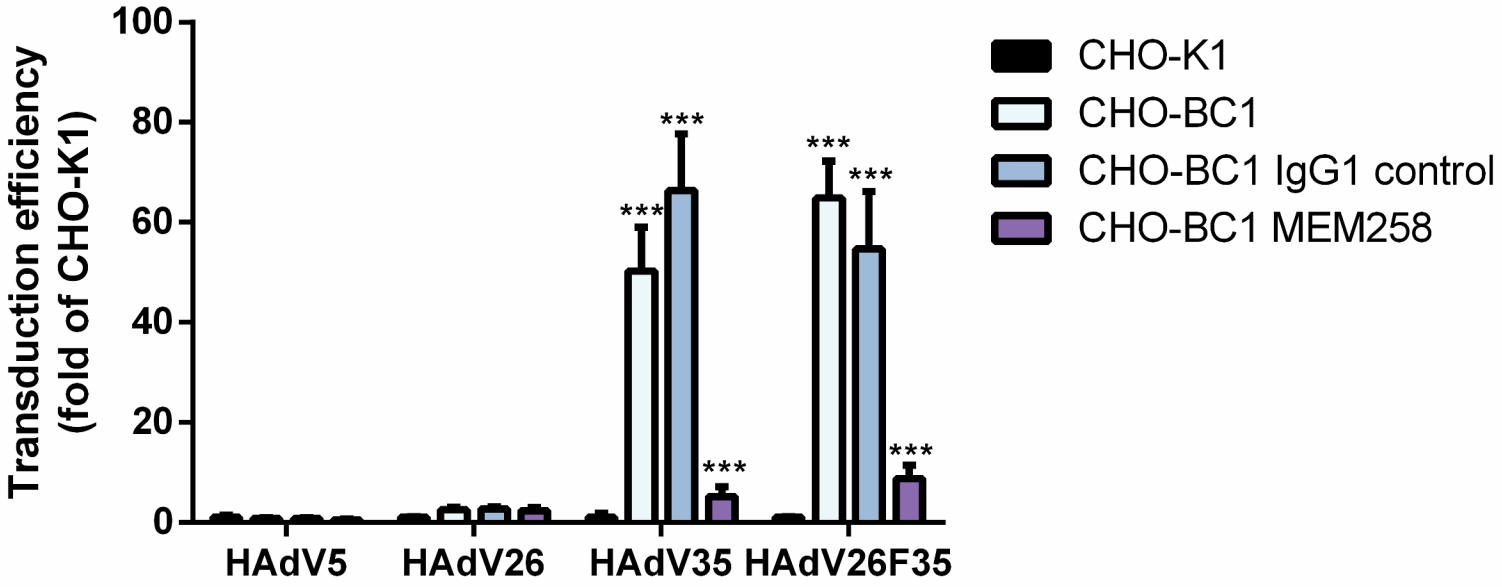
Transduction efficiency
(fold of CHO-K1)
100
80
60
40
20
0
***
***
***
***
***
***
HAdV5
HAdV26
HAdV35
HAdV26F35
CHO-K1
CHO-BC1
CHO-BC1 IgG1 control
CHO-BC1 MEM258

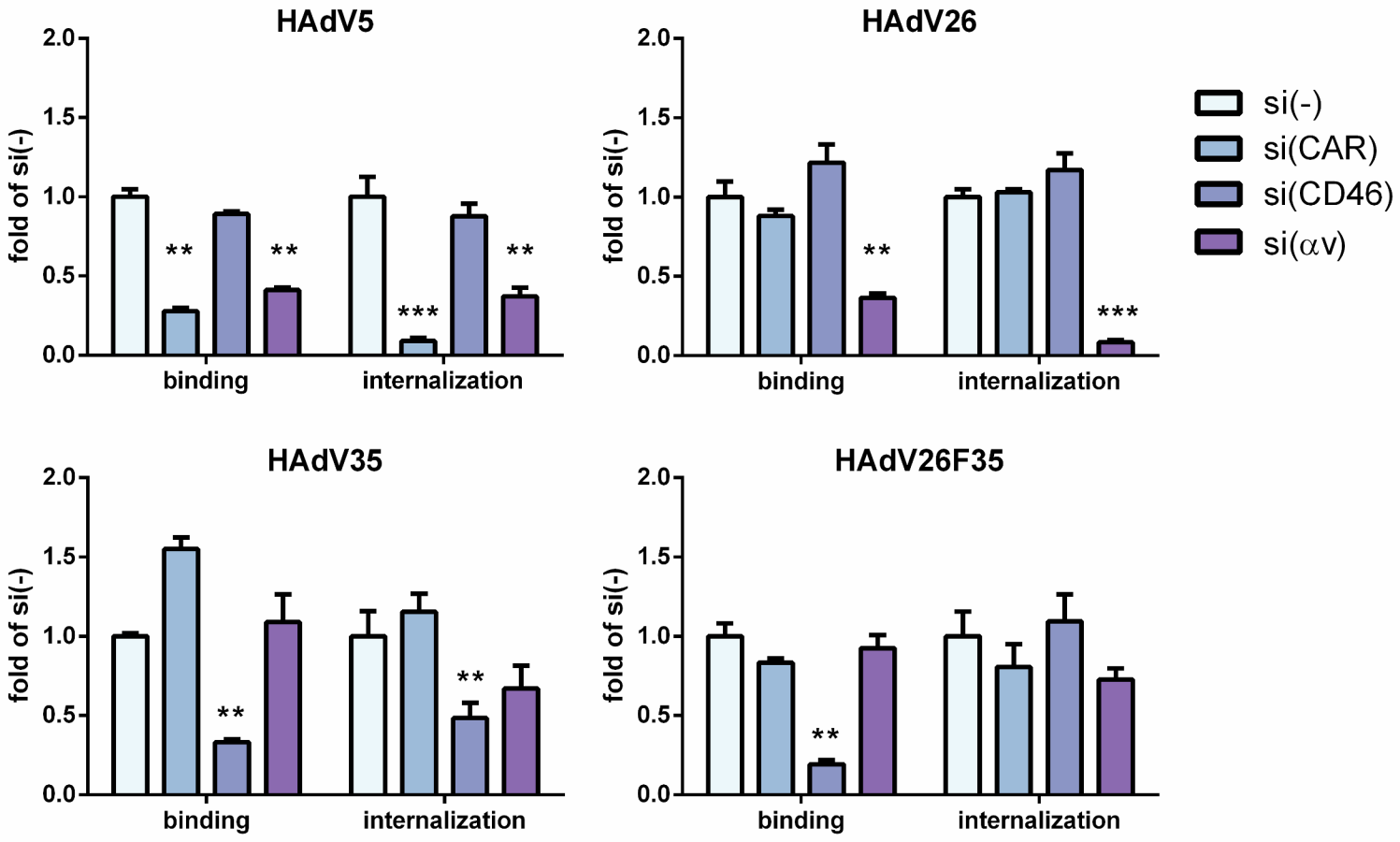
HAdV5
HAdV26
HAdV35
HAdV26F35
fold of si(-)
2.0
1.5
1.0
0.5
0.0
**
***
binding
internalization
si(-)
si(CAR)
si(CD46)
si(αv)

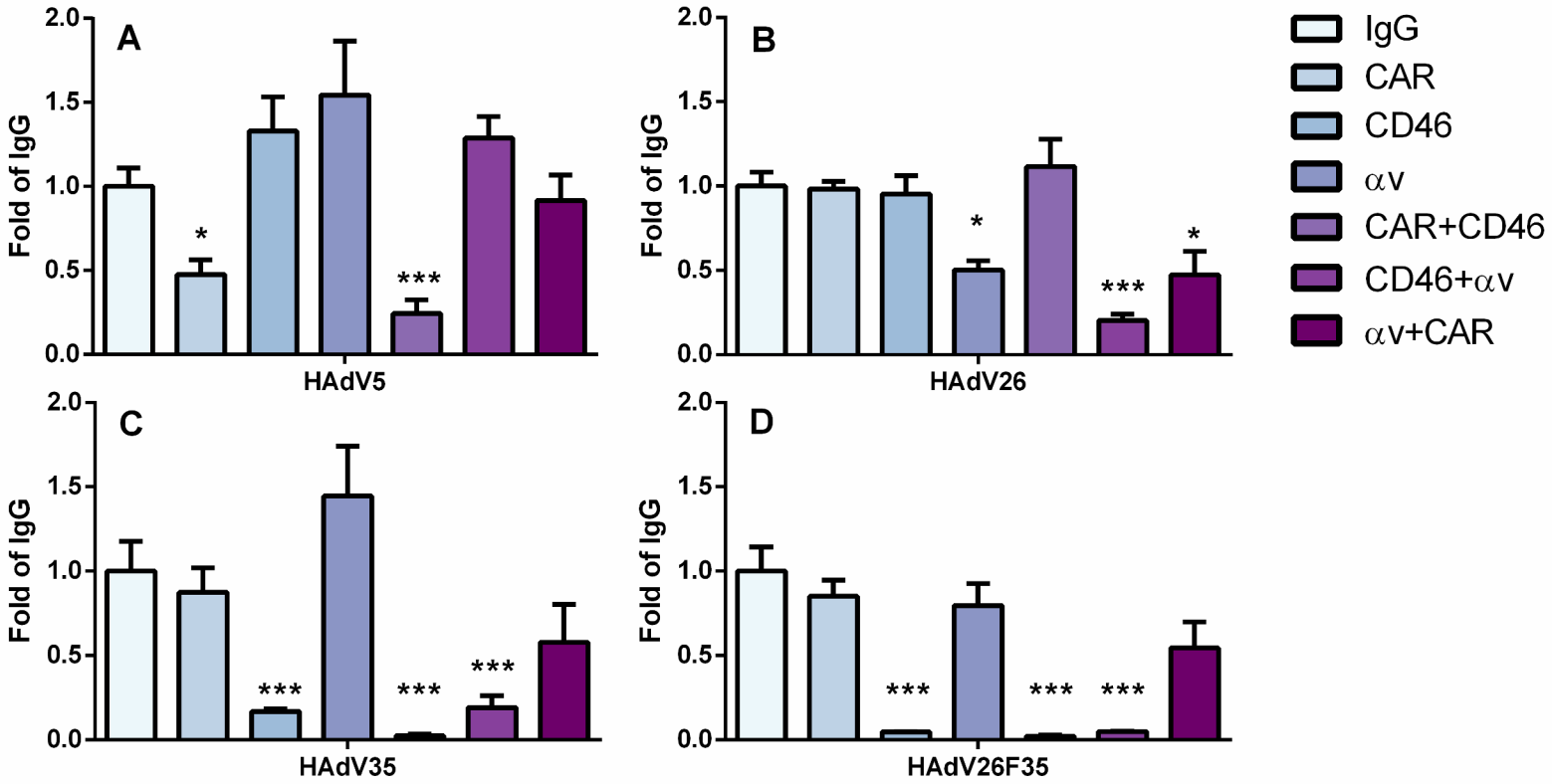
A
B
C
D
Fold of IgG
2.0
1.5
1.0
0.5
0.0
*
***
HAdV5
HAdV26
HAdV35
HAdV26F35
IgG
CAR
CD46
αv
CAR+CD46
CD46+αv
αv+CAR

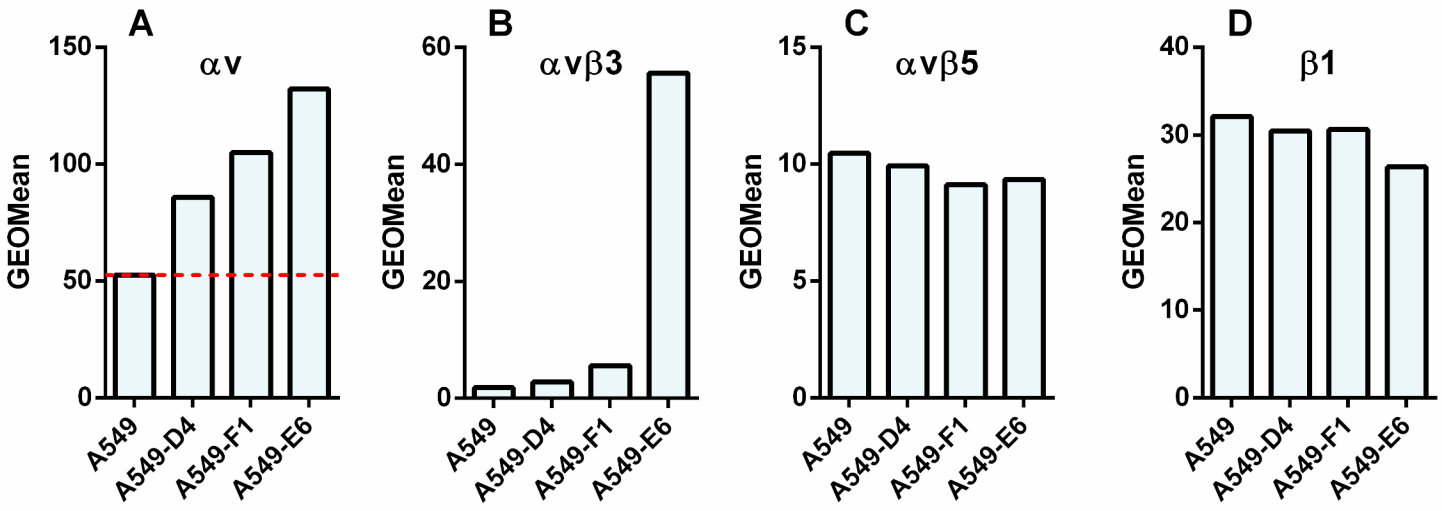
A
αv
GEOMean
150
100
50
0
A549
A549-D4
A549-F1
A549-E6
B
αvβ3
GEOMean
60
40
20
0
A549
A549-D4
A549-F1
A549-E6
C
αvβ5
GEOMean
15
10
5
0
A549
A549-D4
A549-F1
A549-E6
D
β1
GEOMean
40
30
20
10
0
A549
A549-D4
A549-F1
A549-E6

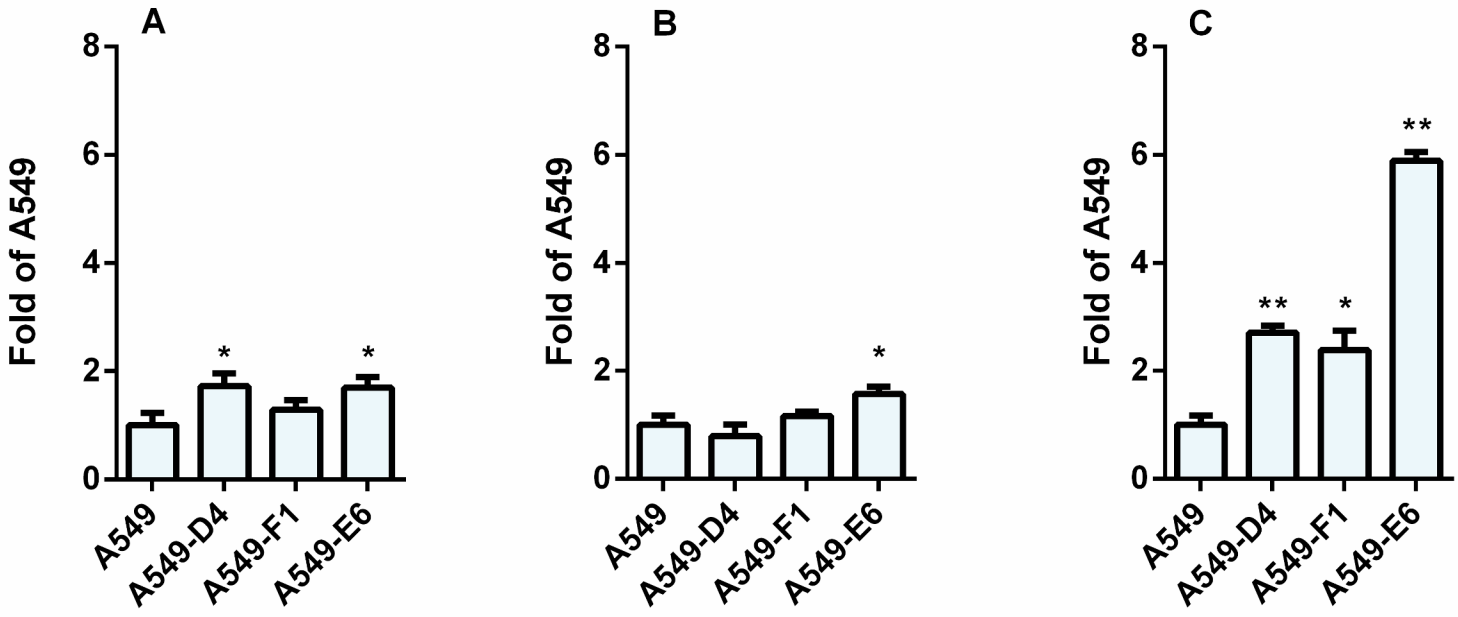
A
B
C
Fold of A549
0
2
4
6
8
*
**
A549
A549-D4
A549-F1
A549-E6

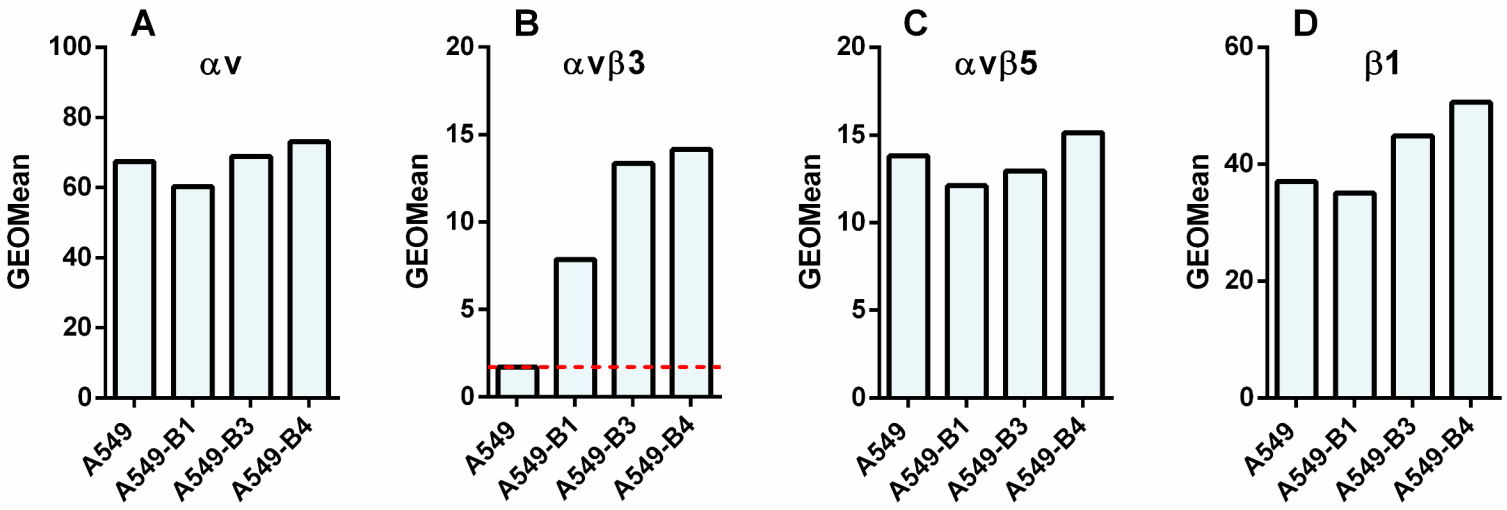
A
αv
GEOMean
100
80
60
40
20
0
A549
A549-B1
A549-B3
A549-B4
B
αvβ3
GEOMean
20
15
10
5
0
A549
A549-B1
A549-B3
A549-B4
C
αvβ5
GEOMean
20
15
10
5
0
A549
A549-B1
A549-B3
A549-B4
D
β1
GEOMean
60
40
20
0
A549
A549-B1
A549-B3
A549-B4

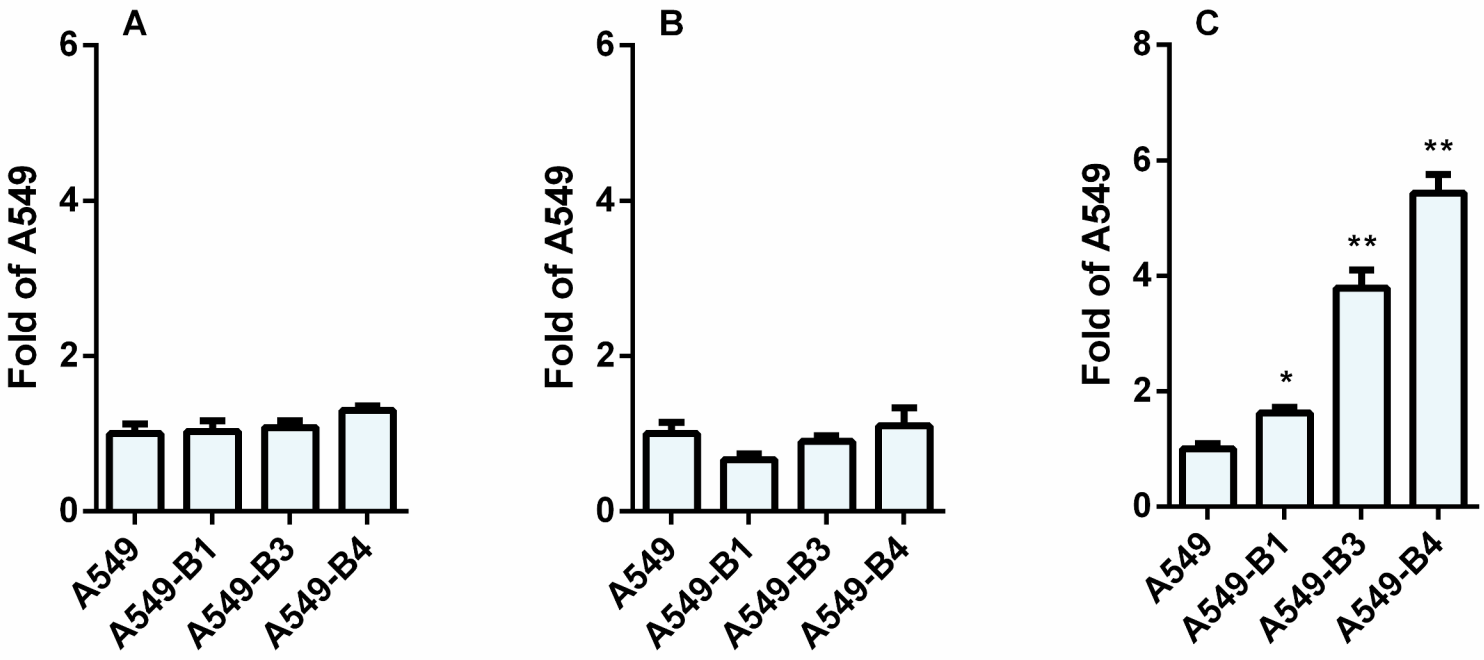
A
B
C
Fold of A549
0
2
4
6
8
*
**
A549
A549-B1
A549-B3
A549-B4

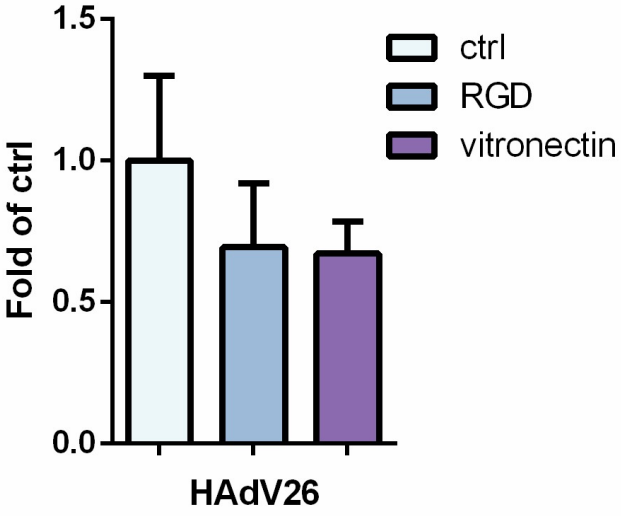
1.5
1.0
0.5
0.0
Fold of ctrl
ctrl
RGD
vitronectin
HAdV26

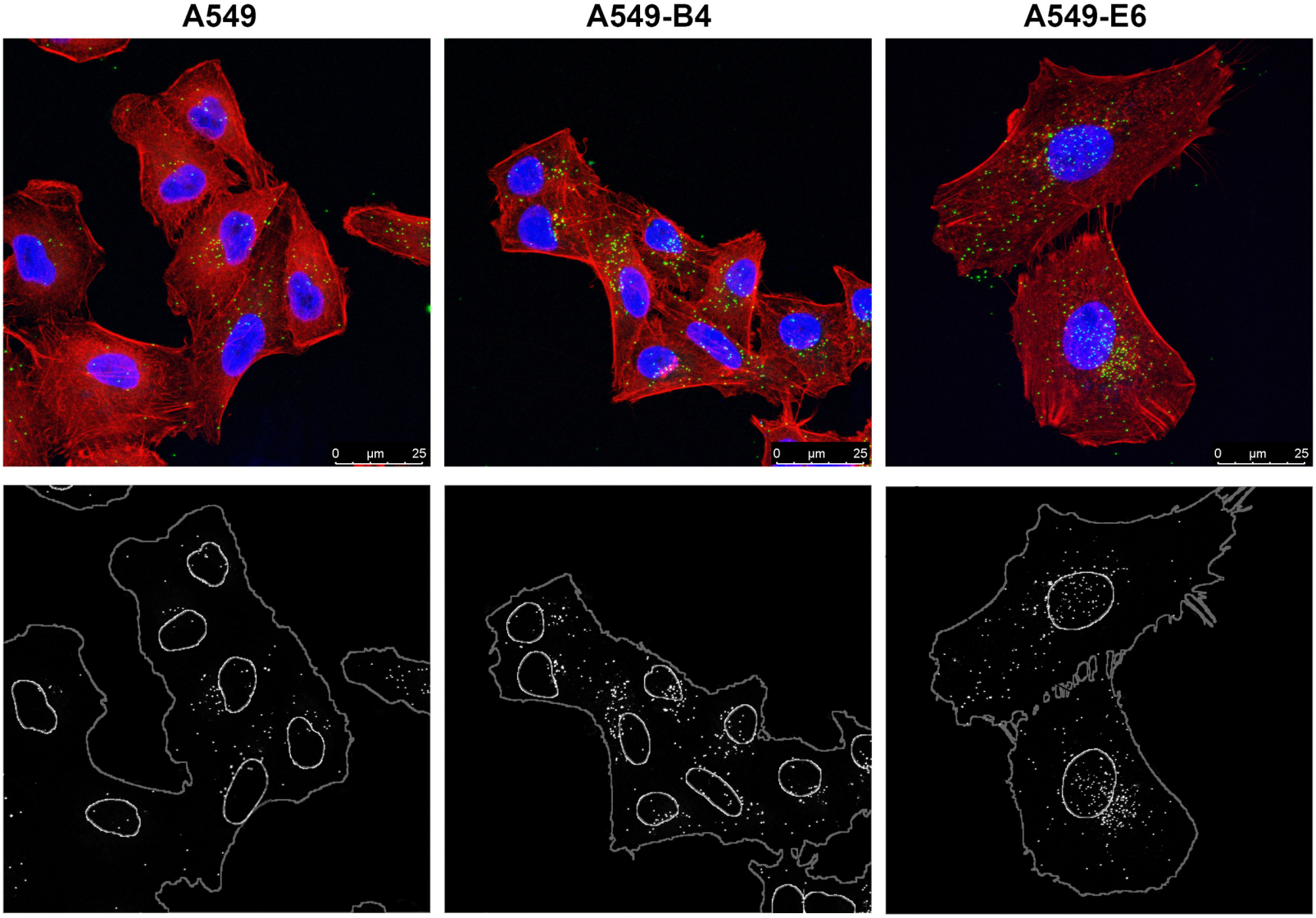
A549
A549-B4
A549-E6
0 µm 25
0 µm 25
0 µm 25

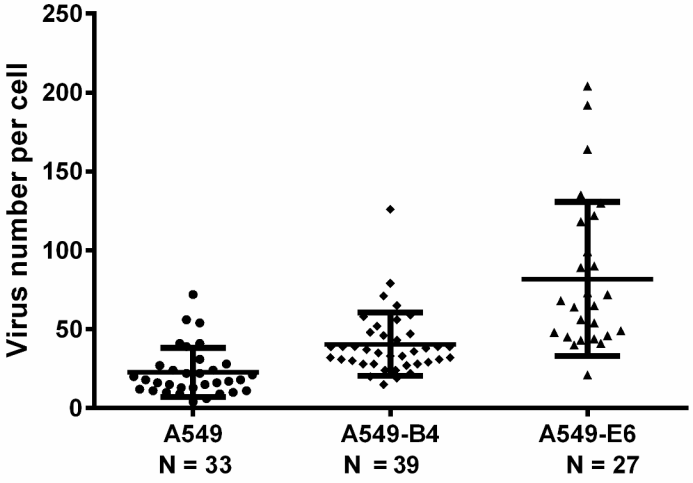
Virus number per cell
250
200
150
100
50
0
A549
N = 33
A549-B4
N = 39
A549-E6
N = 27

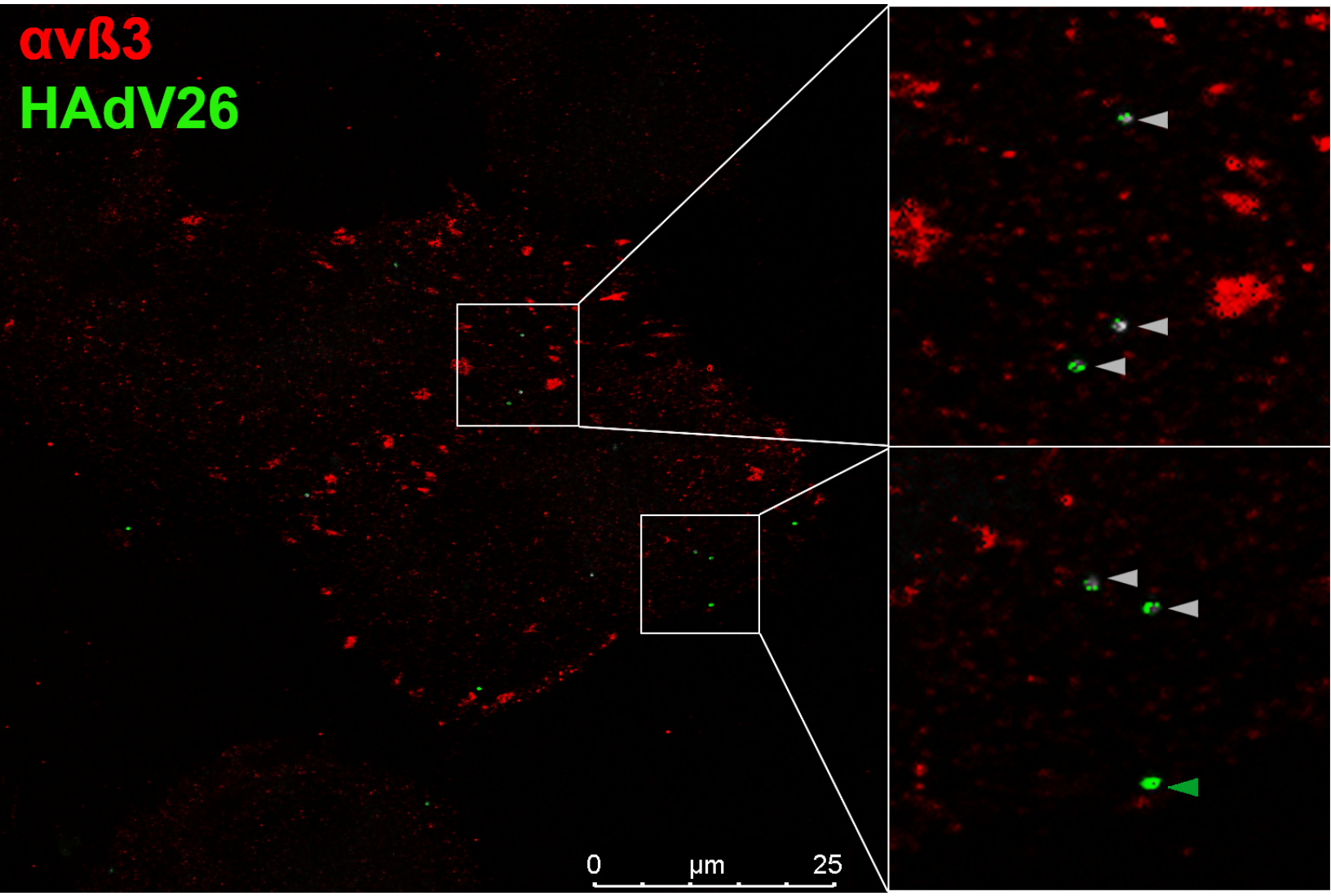
αvß3
HAdV26
0
µm
25

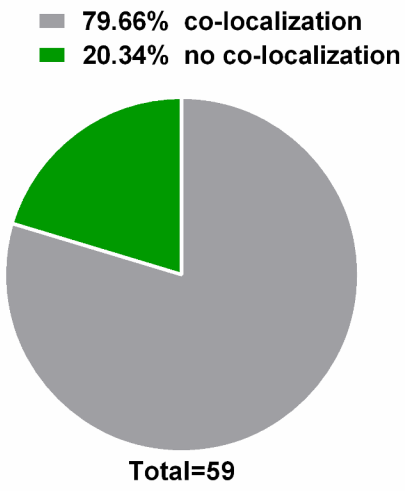
79.66% co-localization
20.34% no co-localization
Total=59